

## General Disclaimer

### One or more of the Following Statements may affect this Document

- This document has been reproduced from the best copy furnished by the organizational source. It is being released in the interest of making available as much information as possible.
- This document may contain data, which exceeds the sheet parameters. It was furnished in this condition by the organizational source and is the best copy available.
- This document may contain tone-on-tone or color graphs, charts and/or pictures, which have been reproduced in black and white.
- This document is paginated as submitted by the original source.
- Portions of this document are not fully legible due to the historical nature of some of the material. However, it is the best reproduction available from the original submission.

NASA CR 120851  
BOEING D3-8611-3



# ACOUSTIC RADIATION FROM LINED, UNFLANGED DUCTS – DUCT TERMINATION IMPEDANCE PROGRAM

BY  
R. J. BECKEMEYER AND D. T. SAWDY

DECEMBER 12, 1971  
THE **BOEING** COMPANY  
WICHITA DIVISION - WICHITA, KANSAS, 67210

(NASA-CR-120851) ACOUSTIC RADIATION FROM  
LINED, UNFLANGED DUCTS: DUCT TERMINATION  
IMPEDANCE PROGRAM (Boeing Co., Wichita,  
Kans.) 77 p HC \$4.75

CSCL 20A

Unclassified  
N75-28851  
G3/71  
29848



PREPARED FOR  
NATIONAL AERONAUTICS AND SPACE ADMINISTRATION

NASA-LEWIS RESEARCH CENTER  
CONTRACT NAS 3-14321  
H. BLOOMER, PROJECT MANAGER

NASA CR 120851  
BOEING D3-8611-3

TOPICAL REPORT

ACOUSTIC RADIATION FROM LINED, UNFLANGED DUCTS –  
DUCT TERMINATION IMPEDANCE PROGRAM

by  
R. J. Beckemeyer and D. T. Sawdy

THE BOEING COMPANY  
3801 SOUTH OLIVER  
WICHITA, KANSAS 67210

Prepared For  
NATIONAL AERONAUTICS AND SPACE ADMINISTRATION  
December 12, 1971

CONTRACT NASA 3-14321

NASA-LEWIS RESEARCH CENTER  
CLEVELAND, OHIO  
H. BLOOMER, PROJECT MANAGER  
V/STOL AND NOISE DIVISION

## FOREWORD

The work described herein was done by The Boeing Company, Wichita Division, under NASA contract NAS 3-14321 with Mr. H. Bloomer, V/STOL and Noise Division, NASA - Lewis Research Center, as Project Manager.

## ABSTRACT

An acoustic radiation analysis has been developed to predict the far-field characteristics of fan noise radiated from an acoustically lined unflanged duct. This analysis is comprised of three modular digital computer programs which together provide a capability of accounting for the impedance mismatch at the duct exit plane. This report discusses the Duct Termination Impedance Program whose relationship with the other two modular reports of the analyses is illustrated on the following page.

Admissible duct configurations include circular or annular, with or without an extended centerbody. This variation in duct configurations provides a capability of modeling inlet and fan duct noise radiation.

DEVELOPMENT OF ACOUSTIC RADIATION ANALYSIS  
OF TURBOFAN NOISE FROM LINED, UNFLANGED DUCTS

OVERALL DOCUMENT ORGANIZATION

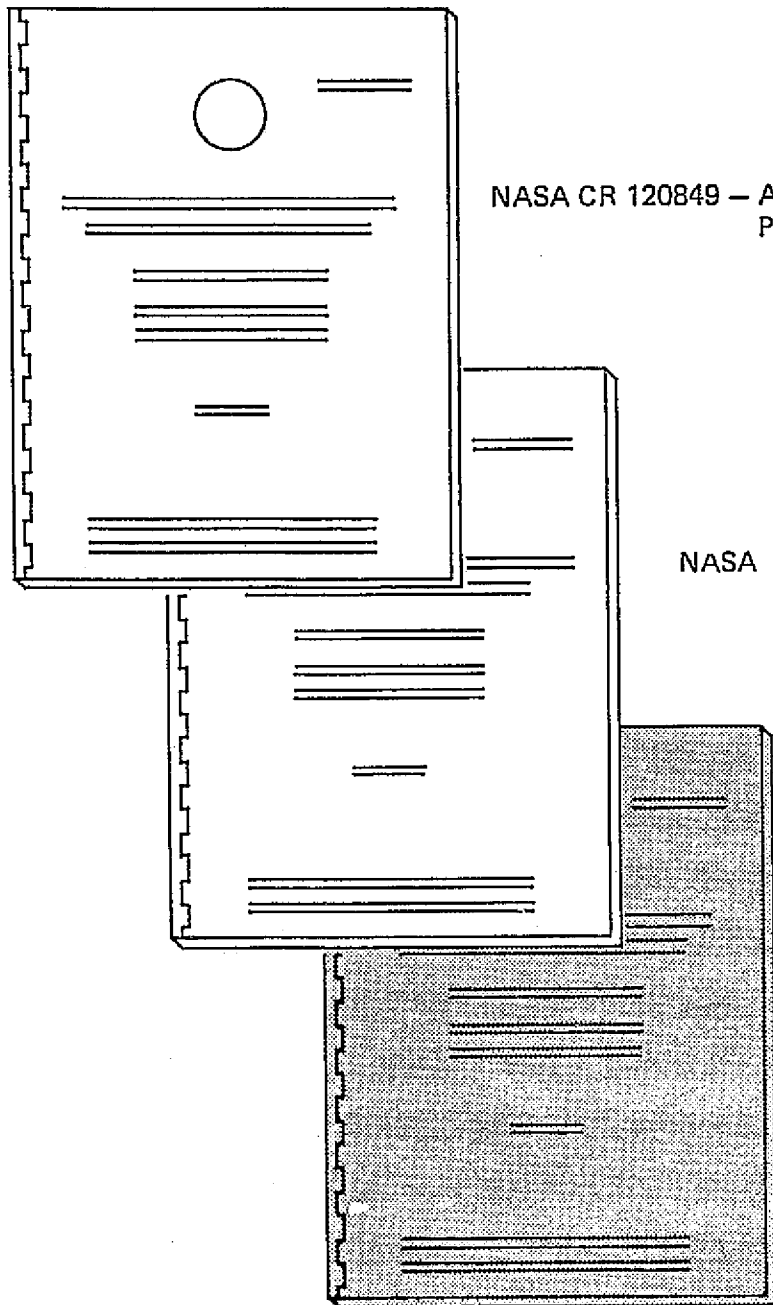


## TABLE OF CONTENTS

	PAGE
NOMENCLATURE . . . . .	vi
INDEX OF FIGURES . . . . .	vii
1.0 INTRODUCTION . . . . .	1
1.1 Background . . . . .	1
1.2 Technical Approach . . . . .	1
2.0 MATHEMATICAL DEVELOPMENT . . . . .	3
3.0 METHOD OF SOLUTION . . . . .	7
4.0 RESULTS . . . . .	11
4.1 Application . . . . .	11
4.2 Limitations . . . . .	11
5.0 CONCLUSIONS AND RECOMMENDATIONS . . . . .	13
6.0 REFERENCES . . . . .	15
7.0 FIGURES . . . . .	17
APPENDIX 1 – PROGRAM DESCRIPTION . . . . .	23
Nomenclature	
Input	
Program Flow	
Output	
APPENDIX 2 – PROGRAM FLOW CHARTS . . . . .	29
APPENDIX 3 – MAIN PROGRAM LISTING . . . . .	41
APPENDIX 4 – PRES0 SUBROUTINE LISTING . . . . .	45
APPENDIX 5 – PRES1 SUBROUTINE LISTING . . . . .	49
APPENDIX 6 – PRES2 SUBROUTINE LISTING . . . . .	53
APPENDIX 7 – GAUSS SUBROUTINE . . . . .	57
APPENDIX 8 – EXAMPLE PROBLEM . . . . .	63
Listing of Input Data	
Output for Example Problem	

## NOMENCLATURE

### Analytical Variables

a	Centerbody Radius
b	Outer Duct Radius
c	Sound Speed in Air
I	Acoustic Intensity
k	Wave number, $k = \omega/c$
m	Angular Mode No.
r	Radial Coordinate
$r_j$	Radial Coordinate Integration Variable
R	Distance between Points
$R_j$	Distance between Point on Duct & Field Point
t	Time
u	Radial Velocity Component
v	Axial Velocity Component
V	Velocity Distribution on Exit Face
z	Axial Coordinate
Z	Modal Impedance
$\theta$	Angular Coordinate
$\theta_j$	Angular Coordinate Integration Variable
$\Pi$	Total Sound Power
$\rho$	Air Density
$\tau$	Radiation Resistance
$\phi$	Velocity Potential
$\Phi_j$	Source Strength Distribution
X	Radiation Reactance
$\omega$	Frequency, Radians/Second

## INDEX OF FIGURES

<u>FIGURE</u>		<u>PAGE</u>
1	Possible Duct Configurations . . . . .	19
2	Geometry . . . . .	20
3	Box Method Integration and Control Blocks . . . . .	21
4	Pressure Distribution on Duct Exit Plane . . . . .	22

## 1.0 INTRODUCTION

### 1.1 Background

This report discusses the Duct Termination Impedance Program that forms the intermediate link for the package of modular computer programs which together form a first generation capability for the analytical prediction of far-field noise being radiated from an unflanged inlet or exhaust duct.

The development of this program had its origin in the need for a method to correct the far-field directivity patterns for the discontinuity in the duct impedance that exists at the duct termination. It is known that when a propagating wave traverses the duct exit plane that part of the energy is reflected back up the duct while the remainder is transmitted through the interface. In addition, the radial variation of the termination impedance generates higher radial duct modes. Thus, both reflected and transmitted waves contain modes other than the modes comprising the incident wave. Obviously, it is necessary to understand the concept of modal coupling to determine the amount of energy radiated to the far-field and its modal content.

The subject program couples the infinite space exterior to the duct, to the interior of the duct by accounting for the impedance mismatch at the duct exit plane. This digital program utilizes the output from the Acoustic Source Distribution Program, Reference 1, to generate the pressure distribution and impedance which act on the duct exit plane. This information is then used by the Directivity Index Program, Reference 2, to determine the far-field radiation patterns for a semi-infinite length duct which are corrected for the impedance mismatch at the duct exit plane.

### 1.2 Technical Approach

This technical development is concerned with the effect of the impedance mismatch at the duct exit plane on the radiation of fan or compressor noise from an inlet or exhaust duct. Admissible duct configurations, shown in Figure 1, include unflanged circular or annular ducts, with or without extended centerbodies.

The approach presented here is an extension of the case of the radiation of sound from a duct with an infinite baffle on its end to the unflanged case which accounts for the diffraction of sound around the outside lip of the duct. Phased contributions of the outer and extended inner duct surfaces and the duct exit plane must be determined and then combined to determine the total pressure acting on the open face.

The duct termination impedance characteristics of the duct configuration are determined from the spatial distributions of acoustic sources over the duct walls and exit plane. The source distribution which satisfies the imposed boundary conditions is determined by the Acoustic Source Distribution Program, Reference 1. These boundary conditions require that the acoustic perturbation velocity normal to the outer duct walls must vanish. In addition, the normal velocity distribution over the duct exit plane must equal

the velocity distribution associated with either a single mode or a combination of modes of discrete frequency.

The acoustic source strengths are numerically integrated over the duct walls and exit plane to yield the pressure distribution on the duct face. From the calculated pressure distribution and the known velocity distribution, two impedances are calculated. The first is a localized or point impedance which is defined as the ratio of the pressure on a given segment on the duct face to the velocity on that segment. This distributed or local impedance reflects the modal coupling effects of the impedance mismatch at the open end of the duct. The second impedance is a modal impedance which is constant across the duct face and provides a measure of the radiation efficiency of the given velocity distribution.

Several assumptions have been made in this development. These concern the transport characteristics of the model and the decomposition of the acoustic sound energy into the acoustic modes present in the duct. The acoustic sound is assumed to be radiated through an ideal fluid (nonviscous) which has no mean flow. This simplification will not significantly affect the results for noise propagation through a locally subsonic flow field of an inlet. However, radiation through an exhaust or jet flow will not be represented properly by this model.

The velocity distribution is assumed to have a  $\cos(m\theta)$  type of angular dependence. This simplification is justified by the angular characteristic functions determined from the solution of the governing wave equation for sound propagation through annular ducts. This assumption does not affect the ability to couple different modes in the far-field program, Reference 2, but does restrict this program to the extent that for a velocity distribution whose angular dependence is specified by a combination of different  $m$  angular modes, a separate analysis must be made for each set of angular modes.

## 2.0 MATHEMATICAL DEVELOPMENT

The acoustic pressure on the open face of an unflanged duct is formulated in terms of the acoustic velocity potential. This formulation provides a mathematical model with a straightforward method of satisfying the velocity boundary conditions on the duct walls and exit plane. The phase of the pressure wave transmitted through the duct exit plane is accounted for in the phase relationship of the potential function.

Since the velocity potential is governed by a linear set of equations, superposition may be used to determine the field potential  $\phi$  in the region exterior to the duct. The potential for the mathematical model shown in Figure 2, is determined by the superposition of three potentials  $\phi_0$ ,  $\phi_1$ ,  $\phi_2$ , which represent the contribution of the duct face, outer duct wall and extended centerbody duct wall, respectively. This technique is expressed mathematically by

$$\phi(r, \theta, z, t) = \phi_0 + \phi_1 + \phi_2 \quad (1)$$

The component velocity potentials are determined by a spatial distribution of monopole acoustic sources on each reflecting surface. For example, the velocity potential due to a distribution of harmonically vibrating sources on the face of the duct is

$$\phi_0 = e^{-i\omega t} \int_0^{2\pi} \int_a^b \frac{\Phi_0(r_0) e^{i\omega R_0/c}}{R_0} \cos(m\theta_0) r_0 d\theta_0 dr_0 \quad (2)$$

The form of this integral equation is derived from the following assumptions:

- Acoustic velocity at the point P may be determined from a monopole acoustic source  $e^{-i(\omega t - kR_0)}/R_0$ , which represents an outward propagating wave and is a solution of the wave equation in spherical coordinates.
- The angular dependence of the potential may be described in terms of the characteristic function  $\cos(m\theta)$  for a given angular mode number m.
- The radial distribution of sources is given by the spatial distribution function  $\Phi_0(r)$  which is determined by the Acoustic Source Distribution Program, Reference 1.

Similarly, the velocity potential terms for the outer and extended inner duct wall surfaces, respectively, are

$$\phi_1 = e^{-i\omega t} \int_{-\infty}^0 \int_0^{2\pi} \frac{\Phi_1(z_1) e^{i\omega R_1/c}}{R_1} \cos(m\theta_1) d\theta_1 b dz_1, \quad (3)$$

$$\phi_2 = e^{-i\omega t} \int_0^\infty \int_0^{2\pi} \frac{\Phi_2(x_2)}{R_2} e^{i\omega R_2 t} \cos(m\theta_2) d\theta_2 dx_2 \quad (4)$$

Acoustic pressure is related to the velocity potential by

$$p = \rho \frac{\partial \phi}{\partial r}$$

The velocity potential of Equation (1) yields the following expression for pressure varying harmonically.

$$p = -i\omega\rho \left\{ \phi_0 + \phi_1 + \phi_2 \right\} \quad (5)$$

To determine the pressure at the point  $r, \theta$  on the open face of the duct, the separation distances in Equations (2) through (4) are

$$R_j = \sqrt{(r \cos \theta - \lambda_j \cos \theta_j)^2 + (r \sin \theta - \lambda_j \sin \theta_j)^2} \quad (6)$$

where  $j = 0, 1, 2$

$$\lambda_0 = r_0$$

$$\lambda_1 = b$$

$$\lambda_2 = a$$

A useful quantity in the study of sound radiation from ducts is the modal impedance in the axial direction. The modal impedance at the duct exit plane is defined in terms of the acoustic pressure and velocity, in any mode, which are present on the duct exit plane.

$$\bar{Z} = \frac{p}{v}$$

The modal impedance which is expressed mathematically as a complex quantity, is written in terms of its real and imaginary parts which are normalized by the specific impedance of air  $\rho c$ , by

$$\bar{Z} = \rho c (\tau - iX) \quad (7)$$

The variable  $\tau$  is the radiation resistance which is a measure of acoustic energy radiated through the exit plane and the variable  $X$  is the radiation reactance which is a measure of the acoustic energy reflected back up the duct.

Acoustic pressure and velocity are related to the impedance through the sound intensity radiated through the duct exit plane. In a stationary medium, the sound intensity is defined to be the time average of pressure times velocity. Mathematically, the intensity is

related to the real part of the product of the complex conjugate of the pressure and velocity by

$$I = \frac{1}{2} \operatorname{Re}(p^* v) \quad (8)$$

Sound intensity, normal to an area, is the rate at which the sound energy crosses a unit of that area. Thus, the total sound power radiated through the duct exit is

$$P = \int_a^b \int_0^{2\pi} I r_0 dr_0 d\theta_0 \quad (9)$$

Sound intensity is related to the impedance by two expressions; one which involves only the radiation resistance

$$I = \frac{1}{2} \rho_c \tau |v|^2$$

and the other which includes the radiation reactance.

$$I = \frac{1}{2} \frac{\tau |p|^2}{\rho_c (\tau^2 + X^2)}$$

These expressions are substituted into Equation (9) and the resulting expressions for radiated energy are equated to yield the following relations for the impedance:

$$\tau = \frac{1}{\rho_c} \frac{\iint \operatorname{Re}(p^* v) r_0 dr_0 d\theta_0}{\iint |v|^2 r_0 dr_0 d\theta_0} \quad (10)$$

$$X^2 = \frac{1}{(\rho_c)^2} \frac{\iint |p|^2 r_0 dr_0 d\theta_0}{\iint |v|^2 r_0 dr_0 d\theta_0} - \tau^2 \quad (11)$$

### 3.0 METHOD OF SOLUTION

The constraint on this program to be compatible with the Acoustic Source Distribution Program of Reference 1, required that the "Box Method" technique be used to solve Equations (2) through (4). This mathematical technique assumes that the variation of the source distribution over a small portion or box of the reflecting surface is constant, an assumption which allows the integrations to be evaluated by a summation. To facilitate the numerical solution of these equations, the duct exterior face is divided into a sequence of M annular rings, and the duct walls into N and N2 cylindrical segments as shown in Figure 3.

Application of the box method to  $\phi_0$ , the duct face contribution to exit plane pressure, enables the integral equation to be written as

$$\phi_0 = \sum_{I=1}^M \phi_{0I} \sum_{K=1}^L \int \int \cos(m\theta_0) \frac{e^{i\frac{\omega}{c} R_0}}{R_0} r_0 dr_0 d\theta_0 \quad (12)$$

For the duct wall contributions, the equations become

$$\phi_1 = \sum_{I=1}^N \phi_{1I} \sum_{K=1}^L \int \int \cos(m\theta_1) \frac{e^{i\frac{\omega}{c} R_1}}{R_1} bdz_1 d\theta_1 \quad (13)$$

$$\phi_2 = \sum_{I=1}^{N_2} \phi_{2I} \sum_{K=1}^L \int \int \cos(m\theta_2) \frac{e^{i\frac{\omega}{c} R_2}}{R_2} adz_2 d\theta_2 \quad (14)$$

Equations (12) through (14) are integrated numerically. The numerical technique used is an even order Gaussian quadrature scheme. The integration for each annular segment is performed by an iterative method. An initial even order quadrature is chosen (usually 2nd or 4th order) and the integral evaluated. The order is increased by 2 and the integration repeated.

The two values of the integral are compared. If they agree to within a specified error, the next segment is integrated. If agreement is not obtained, the order is again increased and the procedure repeated up to a specified maximum order. At this point, the last calculated value of the integral is used and the integration procedure passes to the next segment.

The quadrature method used is the Gauss formula for arbitrary intervals,

$$\int_a^b f(x) dx = \frac{b-a}{2} \sum_{j=1}^{NG} f(x_j) w_j \quad (15)$$

*PRECEDING PAGE BLANK NOT FILMED*

This relation states that the integral may be approximated by a summation of NG (the order of the quadrature) evaluations of the function at a prescribed abscissa  $x_j$  which are multiplied by the associated weight  $w_j$ . The abscissae and weights of the Gaussian Quadrature may be found in Reference 3. The referenced abscissae have the normalized range  $-1 < y < 1$  and are related to the arbitrary interval abscissae by

$$x_j = \frac{(b+a)}{2} + \frac{(b-a)}{2} y_j$$

The numerical equations for the evaluation of the contributions of the duct face, outer duct wall and extended centerbody wall to the pressure, denoted by  $p_0$ ,  $p_1$ ,  $p_2$ , respectively, are

$$p_0 = \omega \sum_{I=1}^M \phi_{0I} \sum_{K=1}^L \frac{\Delta r_I r_I \Delta \theta_K}{4} \sum_{j=1}^{NG} \sum_{k=1}^{NG} \left\{ \frac{\cos(m\theta_k)}{R_0} \sin\left(\frac{\omega}{c} R_0\right) - i \frac{\cos(m\theta_k)}{R_0} \cos\left(\frac{\omega}{c} R_0\right) \right\} r_{0j} w_j w_k \quad (16)$$

where the quadrature points are

$$r_{0j} = \frac{\Delta r_I}{2} - \frac{\Delta r_I}{2} x_j \\ \theta_k = \frac{\Delta \theta_K}{2} - \frac{\Delta \theta_K}{2} x_k \\ p_1 = \omega \sum_{I=1}^M \phi_{1I} \sum_{K=1}^L \frac{b \Delta z_I \Delta \theta_K}{4} \sum_{j=1}^{NG} \sum_{k=1}^{NG} \left\{ \frac{\cos(m\theta_k)}{R_1} \sin\left(\frac{\omega}{c} R_1\right) - i \frac{\cos(m\theta_k)}{R_1} \cos\left(\frac{\omega}{c} R_1\right) \right\} w_j w_k \quad (17)$$

$$p_2 = \omega \sum_{I=1}^M \phi_{2I} \sum_{K=1}^L \frac{c \Delta z_I \Delta \theta_K}{4} \sum_{j=1}^{NG} \sum_{k=1}^{NG} \left\{ \frac{\cos(m\theta_k)}{R_2} \sin\left(\frac{\omega}{c} R_2\right) - i \frac{\cos(m\theta_k)}{R_2} \cos\left(\frac{\omega}{c} R_2\right) \right\} w_j w_k \quad (18)$$

The acoustic pressure distribution on the duct face is determined by performing the operations of Equation (5) for each annular ring.

$$p_I = \rho(p_0 + p_1 + p_2)_I$$

In the evaluation of  $p_0$ , the integral  $\cos(\frac{\omega}{c}R_0)/R_0$  in Equation (16) is nearly singular when the integration is performed over the box containing the control point. The effect of this singularity on the numerical quadrature is a degradation in its convergence. If the error resulting from a low order quadrature is not acceptable, either a higher order quadrature or a closed form evaluation of Equation (16) must be used.

In view of the extremely poor convergence of the quadrature in Equation (16), a closed form approximation of the integral was used. A technique was developed that consisted of removing the singularity by a change of variables and using the series expansion for the exponential function. The excellent convergence properties of this approximation required only a small number of terms. This integral equation is approximated by

$$\begin{aligned} -i\omega \iint_{\Delta r \Delta \theta} \frac{e^{i(\frac{\omega}{c}R_0)}}{R_0} r dr d\theta &\approx \\ 2 \left( \frac{\omega A}{c} \right)^2 \tan \alpha \Gamma_{R_1} + 2 \left( \frac{\omega B}{c} \right)^2 \cot \alpha \Gamma_{R_2} \\ -i \left\{ 2 \omega A \ln \left[ \frac{\sec \alpha + \tan \alpha}{\sec \alpha - \tan \alpha} \right] \Gamma_{I_1} - 2 \left( \frac{\omega A}{c^2} \right)^3 \tan \alpha \sec \alpha \Gamma_{I_2} \right. \\ \left. + 2 \omega B \ln \left[ \frac{\csc \alpha + \cot \alpha}{\csc \alpha - \cot \alpha} \right] \Gamma_{I_3} - 2 \left( \frac{\omega B}{c^2} \right)^3 \cot \alpha \csc \alpha \Gamma_{I_4} \right\} \end{aligned}$$

where

$$A = \frac{r\Delta\theta}{2}$$

$$B = \frac{\Delta r}{2}$$

$$= \arctan \left[ \frac{\Delta r}{r\Delta\theta} \right]$$

$$WA = \frac{\omega A}{c}$$

$$WB = \frac{\omega B}{c}$$

$\ln$  is the natural logarithm

$$\begin{aligned} \Gamma_{R_1} &= 1 - (WA)^2 (\sec^2 \alpha + 2) / 36 + (WA)^2 [\sec^4 \alpha + 4/3 (\sec^2 \alpha + 2)] / 1800 \\ &\quad - (WA)^6 (\sec^6 \alpha + 6/5 (\sec^4 \alpha + 4/3 (\sec^2 \alpha + 2))) / 141120 \end{aligned}$$

$$\begin{aligned} \Gamma_{R_2} &= 1 - (WB)^2 (\csc^2 \alpha + 2) / 36 + (WB)^4 [\csc^4 \alpha + 4/3 \csc^2 \alpha + 8/3] / 1800 \\ &\quad - (WB)^6 (\csc^6 \alpha + 6/5 (\csc^4 \alpha + 4/3 \csc^2 \alpha + 8/3)) / 141120 \end{aligned}$$

$$\Gamma_{I_1} = 1 - (WA)^2/12 + (WA)^4/320 - (WA)^6/16128$$

$$\Gamma_{I_2} = 1/6 - (WA)^2(\sec^2\alpha + 3/2)/240 + (WA)^4 \frac{(\sec^4\alpha)}{3} + \frac{5}{12} \sec^2\alpha + 5/8)/5040$$

$$\Gamma_{I_3} = 1 - (WB)^2/12 + (WB)^4/320 - (WB)^6/16128$$

$$\Gamma_{I_4} = 1/6 - (WB)^2(\csc^2\alpha + 3/2)/240 + (WB)^4(\csc^4\alpha + \frac{5\csc^2\alpha}{4} + \frac{15}{8})/15120$$

The local impedance for each annular ring is calculated from the acoustic velocity and pressure determined at the duct termination.

$$Z_I = \frac{P_I}{V_I}$$

The radiation resistance and the radiation reactance of the modal impedance are calculated from the numerical form of Equations (10) and (11).

$$\tau = \frac{1}{\rho c} \frac{\sum_{I=1}^M \operatorname{Re}(p^* v)_I (\Delta r_I)^2}{\sum_{I=1}^M |v|_I^2 (\Delta r_I)^2} \quad (19)$$

$$\chi = \frac{1}{\rho c} \sqrt{\frac{\sum_{I=1}^M |p|_I^2 (\Delta r_I)^2}{\sum_{I=1}^M |v|_I^2}} - \tau^2 \rho c^2 \quad (20)$$

## 4.0 RESULTS

### 4.1 Application

The numerical techniques developed in Section 3 are applied to the mathematical representation of the radiation problem developed in the Acoustic Source Distribution Program, Reference 1. Duct segmentation parameters and corresponding source distributions are input to this program to determine the termination impedance characteristics of the duct configuration. Far-field directivity patterns corrected for termination impedance effects are determined for each mode and then combined to yield the total noise signature. In the event both an inlet and fan duct are to be modeled, their respective far-field directivity patterns can be calculated and then combined to yield the total noise signature of the nacelle.

An example duct radiation problem is presented to illustrate the output of this program. A source distribution which was generated by Reference 1 for a plane wave velocity distribution on the face of a circular duct (example problem 1) was input to this program. The resulting pressure distribution for the duct exit plane is shown in Figure 4. Values of pressure which are normalized by the characteristic impedance of air,  $p_c$  are plotted against the radial position of each control box. Behavior of the pressure near the outer duct wall is due to the singular behavior of the source distributions, which is discussed in Reference 1. Since the velocity distribution for a plane wave is uniform across the duct, the resulting local impedance is proportional to the pressure. Thus, the local impedance is shown to vary across the duct cross section. The value of modal impedance that resulted from this analysis is given by its components:

$$T = .520$$

$$X = 1.93$$

### 4.2 Limitations

There are several limitations to this analytical program. First, the effect of mean flow within the duct on the termination impedance has been neglected. Although application of this analysis to a nacelle radiation problem does not yield an exact model, it is anticipated that this simplification will not significantly affect results for noise propagation through a locally subsonic flow field of an inlet. However, radiation through an exhaust or jet flow will not be represented properly by the present analysis.

The second limitation to the program is restriction of the specified velocity distribution on the face of the duct to a  $\cos(m\theta)$  type of angular dependence. This assumption does not affect the capability of the program to combine different  $m$  angular modes in the far-field by superposition of the source distributions. It does, however, restrict this program to the extent that for a velocity distribution whose angular dependence is specified by a combination of different  $m$  angular modes a separate analysis must be made for each set of angular modes.

## 5.0 CONCLUSIONS AND RECOMMENDATIONS

An acoustic radiation analysis has been developed that predicts the angular distribution of acoustic energy in the far-field that is radiated from an unflanged duct. In spite of its many advantages, this acoustic radiation analysis is limited in its range of application. For this reason, this analysis has been relegated to the role of a first generation analysis in a commitment to develop an analytical package which will predict radiation characteristics of a turbofan jet engine. As discussed in Reference 1, the present version of the analysis reaches optimum efficiency when it is applied to low frequency noise radiating from an infinite duct. This and the other limitation due to a  $\text{Cos}(m\theta)$  type of angular dependence of the velocity distribution are an inherent property of the "box method" numerical technique.

A second generation version of the program could avoid these limitations by utilizing a collocation technique of evaluating the integrals of Equations (2) through (4). The primary feature of this technique is that a selected analytical expression is used to represent the source distribution. The time saving feature of the collocation technique is that it requires fewer evaluations of the integrals. The collocation procedure would enable the analysis to handle any combination of angular modes, a result which would remove the angular modal coupling limitation and eliminate the need for a large number of angular boxes.

In addition to the collocation procedure, a second generation version of the analysis should contain a method of accounting for a mean flow within the duct. This method should account for the effects of velocity gradients on the distortion of the radiation field by the jet.

PRECEDING PAGE BLANK NOT FILMED

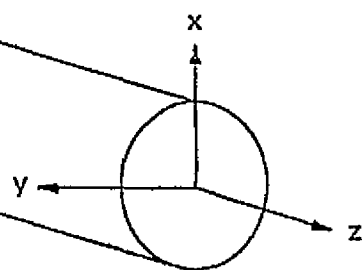
## 6.0 REFERENCES

1. Beckemeyer, R., and Sawdy, D., "Acoustic Radiation from Lined Unflanged Ducts - Acoustic Source Distribution Program," NASA CR 120849, December 1971
2. Beckemeyer, R., and Sawdy, D., "Acoustic Radiation from Lined Unflanged Ducts - Directivity Index Program," Nasa CR 120850, December 1971
3. Abramowitz and Stegun, "Handbook of Mathematical Functions," Dover Publications, 1965.

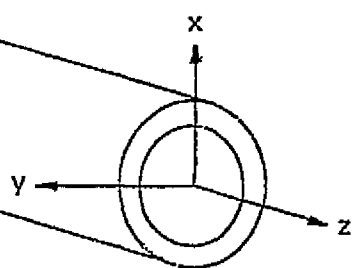
PRECEDING PAGE BLANK NOT FILMED

## **7.0 FIGURES**

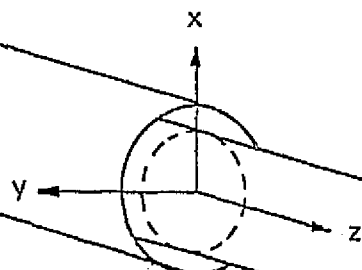
*PRECEDING PAGE BLANK NOT FILMED*



A. Circular Semi-Infinite Duct

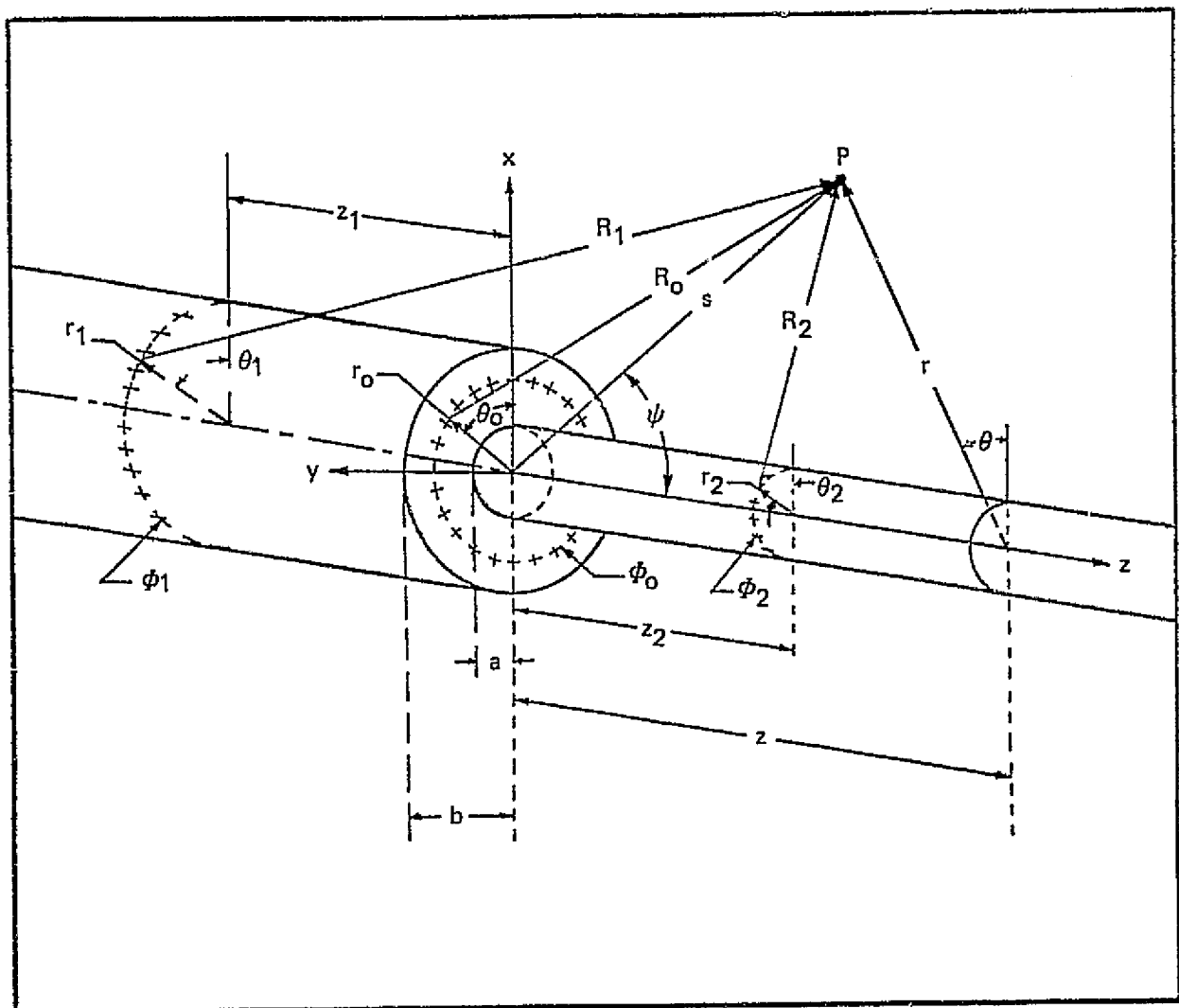


B. Annular Semi-Infinite Duct

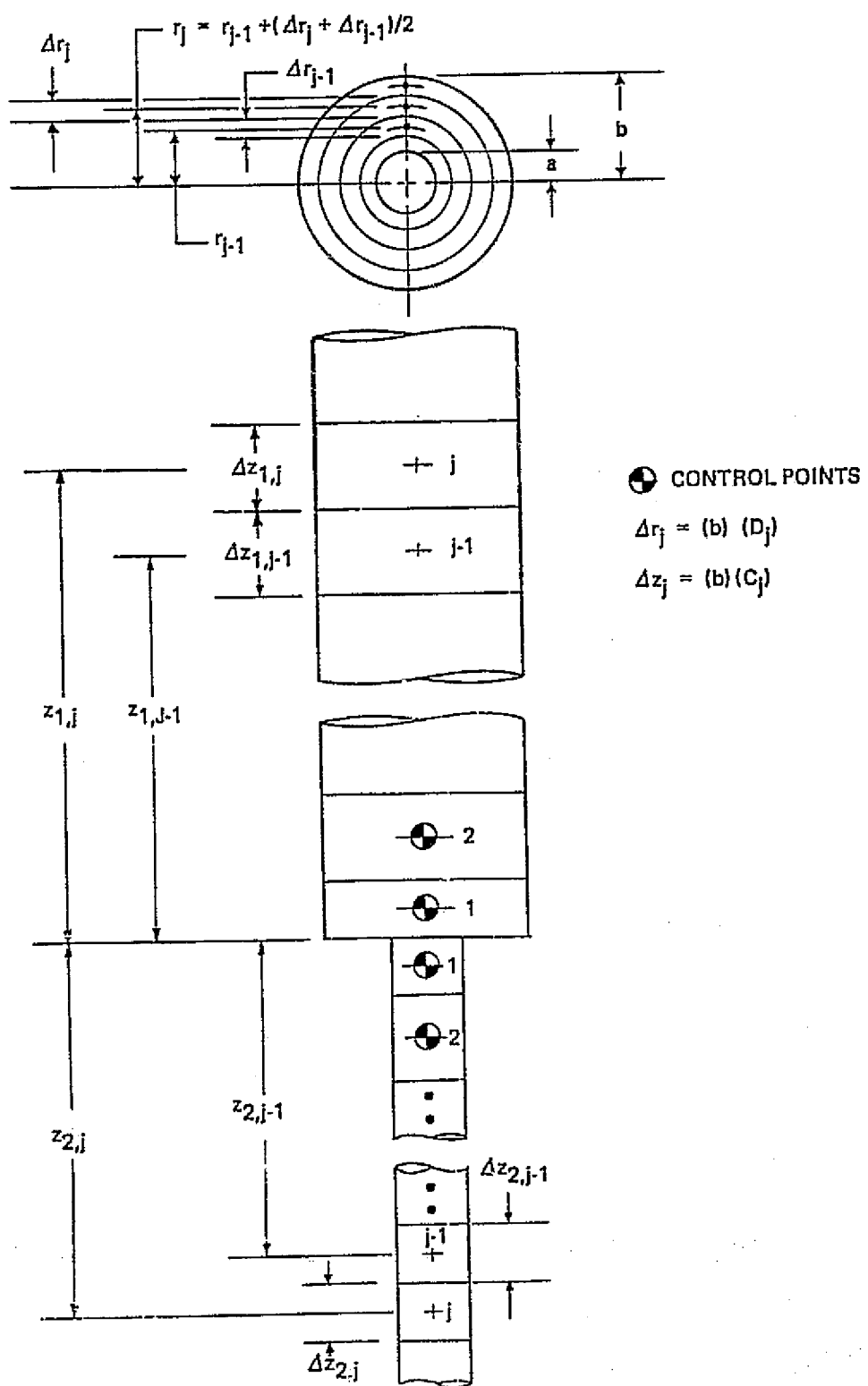


C. Annular Semi-Infinite Duct  
With Infinite Centerbody

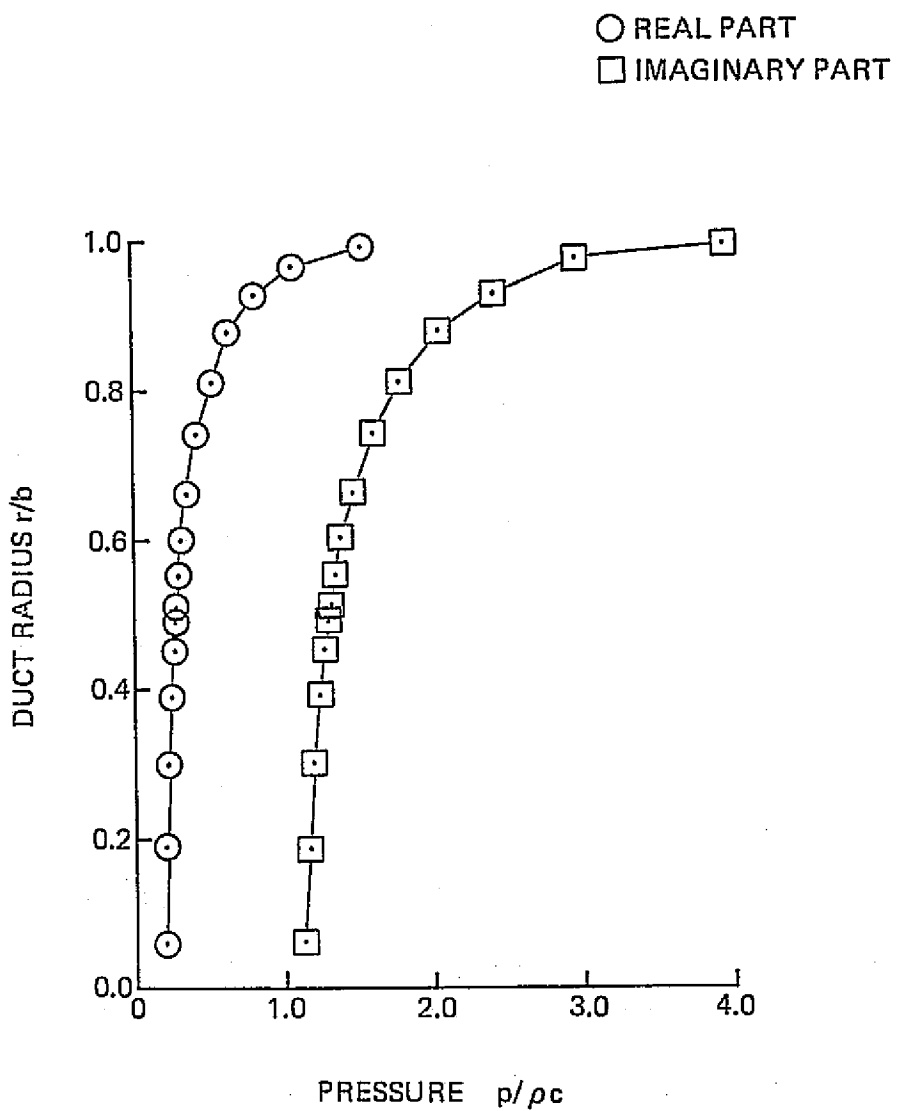
POSSIBLE DUCT CONFIGURATIONS  
FIGURE 1



GEOMETRY  
FIGURE 2



BOX METHOD INTEGRATION AND CONTROL BLOCKS  
FIGURE 3



PRESSURE DISTRIBUTION ON DUCT EXIT PLANE  
FIGURE 4

**APPENDIX 1**  
**PROGRAM DESCRIPTION**

## NOMENCLATURE

### Computer Program Variables

A	Centerbody Radius
ALIMP	Local Impedance
B	Outer Duct Radius
C(I)	Dimensionless Size of Ith Box on Duct Outer Wall
CHI	Radiation Reactance
C2(I)	Dimensionless Size of Ith Box on Extended Centerbody Wall
CHK	Convergency Criterion
D(I)	Dimensionless Size of Ith Box on Duct Exit Face
INK	Configuration Parameter
K	No. of Polar Angles at which Far Field Data is Required
L	No. of Angular Boxes
MW	Angular Mode No.
M	No. of Angular Boxes
N	No. of Cylindrical Boxes on Duct Wall
N2	No. of Cylindrical Boxes on Extended Centerbody Wall
P(I)	Pressure Distribution of Ith Box
PHI(I)	Source Strength Distribution of Ith Box
R	Radial Coordinate
RO,RI	Distance between Point on Duct and Field Point
RHO	Density of Air
S	Sound Speed in Air
TAU	Radiation Resistance
TT	Angular Coordinate
TI	Angular Coordinate Integration Variable
V(I)	Velocity Distribution of Ith Box on Exit Face
W	Frequency Radians/Second
WDS	Wave Number W/S
XANG	Nondimensional Angular Size for Control Box

The basic operation of the Duct Termination Impedance Computer Program is described and the input/output formats are listed. A flow chart of the program is presented in Appendix 2 and listings of the main program and its subroutines are presented in Appendices 3 through 7. An example problem which illustrates the input preparation and output format of the program is presented in Appendix 8.

### INPUT

The input data for the program consists of 23 variables whose symbols and card formats are described below:

<u>CARD OR CARD SET</u>	<u>FORMAT</u>	<u>DATA</u>
1	3612	K      Number of angular points, $\psi$ , at which the directivity index will be calculated.
		M      Number of annular rings used to represent the face of the duct.
		N      Number of cylindrical rings used to represent the outer duct wall.
		N2     Number of cylindrical rings used to represent the extended inner duct wall (if present)
		INK    Indicator for extending the inner duct wall past the duct face. 0 does not extend the wall, 1 extends it to infinity.
		MW     Angular mode number.
	NN	Maximum number of passes to be made through the quadrature iteration loop. NN is related to the highest quadrature order NG by $NN = \frac{NG - 2}{2}$ .
	L	Number of angular segments.
	LP	Number of integrations in integration routine.
	A	Inner duct radius
2	B	Outer duct radius
	W	Circular frequency, radians/second

		S	Speed of sound in units consistent with those of A and B
		CHK	Convergence criteria for numerical integration
		XANG	Nondimensional angular size for control box Radians $= 2\pi(XANG)$ .
		RHO	Air density in units consistent with A, B, and S.
3	6E12.6	C(I), I = 1, N	Outer duct wall box lengths. These lengths are normalized by the outer duct radius, numbered with C(1) closest to the duct exit plane and I increasing in the negative z direction.
4	6E12.6	D(I), I = 1, M	Annular ring box widths. These widths are normalized by the outer duct radius, numbered D(1) at the duct centerline (or adjacent to the centerbody wall duct exit plane intersection) and I increasing to D(M) at the lip of the duct.
5*	6E12.6	C2(I) I = 1, N2	Extended centerbody wall box lengths. These lengths are normalized by the outer duct radius, numbered with C2(1) closest to the duct exit plane and I increasing in the positive z direction.
6	6E12.6	V(I), I = 1, M	Velocity distribution on the duct exit plane. This distribution is numbered with V(1) at the duct centerline (or adjacent to the centerbody wall duct exit plane intersection) and I increasing to V(M) at the lip of the duct.
7	6E12.6	PHIO (I) = 1, M	Source distribution on duct face. Method of numbering this source distribution is analogous to D(I).
8	6E12.6	PHI1(I), I = 1, N	Source distribution on outer duct wall. Method of numbering this source distribution is analogous to C(I).
9*	6E12.6	PHI2(I) I = 1, N2	Source distribution on extended centerbody wall. Method of numbering this source distribution is analogous to C2(I).

\*Card sets 5 and 9 are needed only if INK = 1.

## PROGRAM FLOW

Program operation consists of two separate parts. The first part is a loop which calculates the local pressure distribution and the resulting local impedance. Equations (16) through (18) are solved to yield the exit plane and duct wall contributions  $p_0$ ,  $p_1$ ,  $p_2$  to the pressure distribution on the duct exit plane. The second part calculates the value of the modal impedance. Equations (19) and (20) are solved to yield the resistive and reactive components of the modal impedance.

Four subroutines are required to calculate the pressure distribution on the duct face. PRES0, PRES1, and PRES2 calculate the contribution of exit plane and duct wall contributions to the pressure distribution. GAUSS is the subroutine that provides the weights and abscissae for the Gaussian quadrature described in Equation (15). Listings of PRES0, PRES1, PRES2, and GAUSS are presented in Appendices 4 through 7, respectively.

## OUTPUT

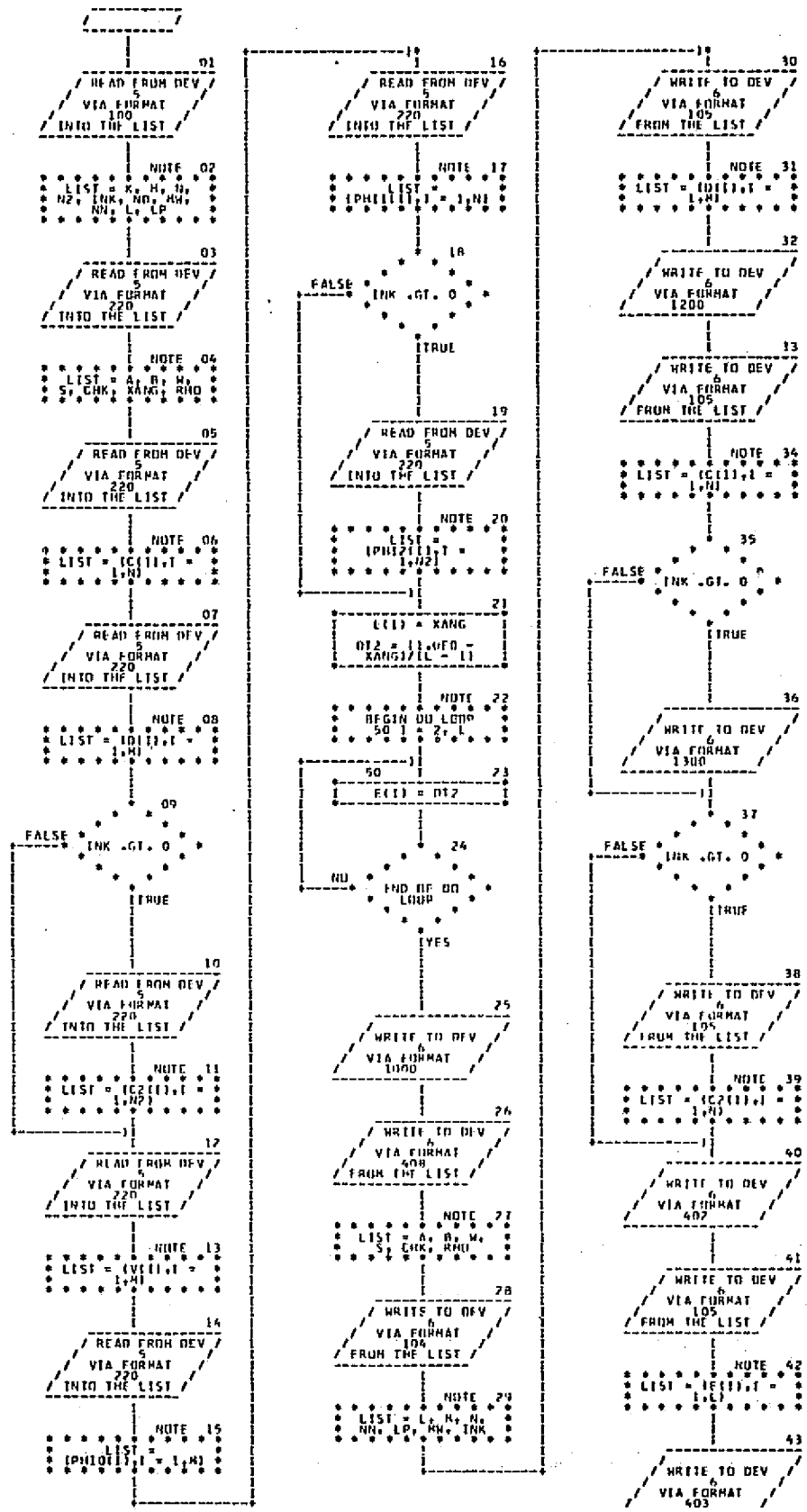
The output format consists of three groups of data:

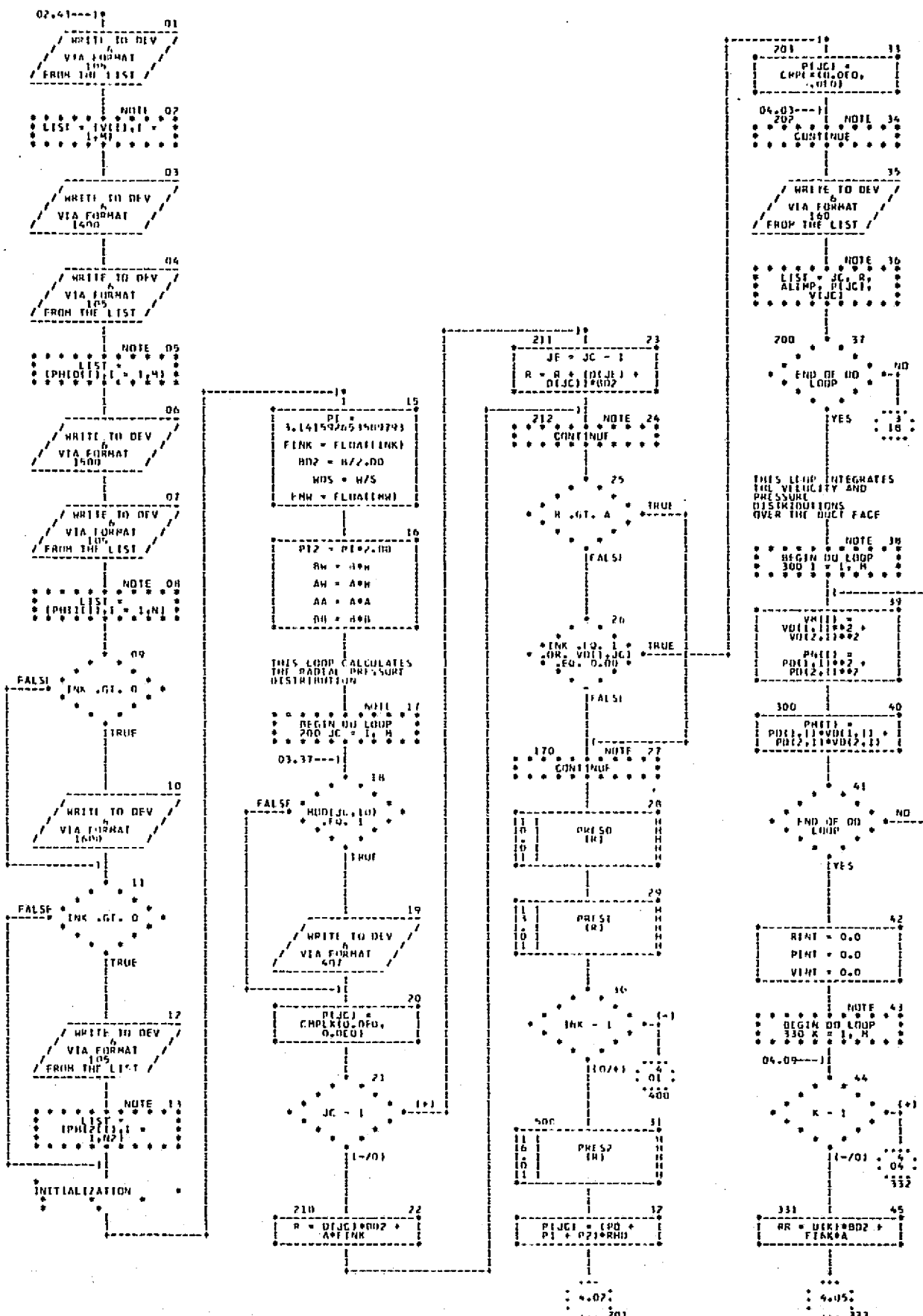
1. Input Data — All pertinent input data are printed out.
2. Distribution of pressure and impedance — Values of local impedance, pressure and velocity for each annular ring and its corresponding radial position are printed out in row format. For each angular integration that fails to meet the convergence criteria, values of angular position, radial position, differences of the real and imaginary parts of the integral are printed out.
3. Modal Impedance — The resistive and reactive parts of the modal impedance are printed.

## **APPENDIX 2**

### **PROGRAM FLOW CHARTS**

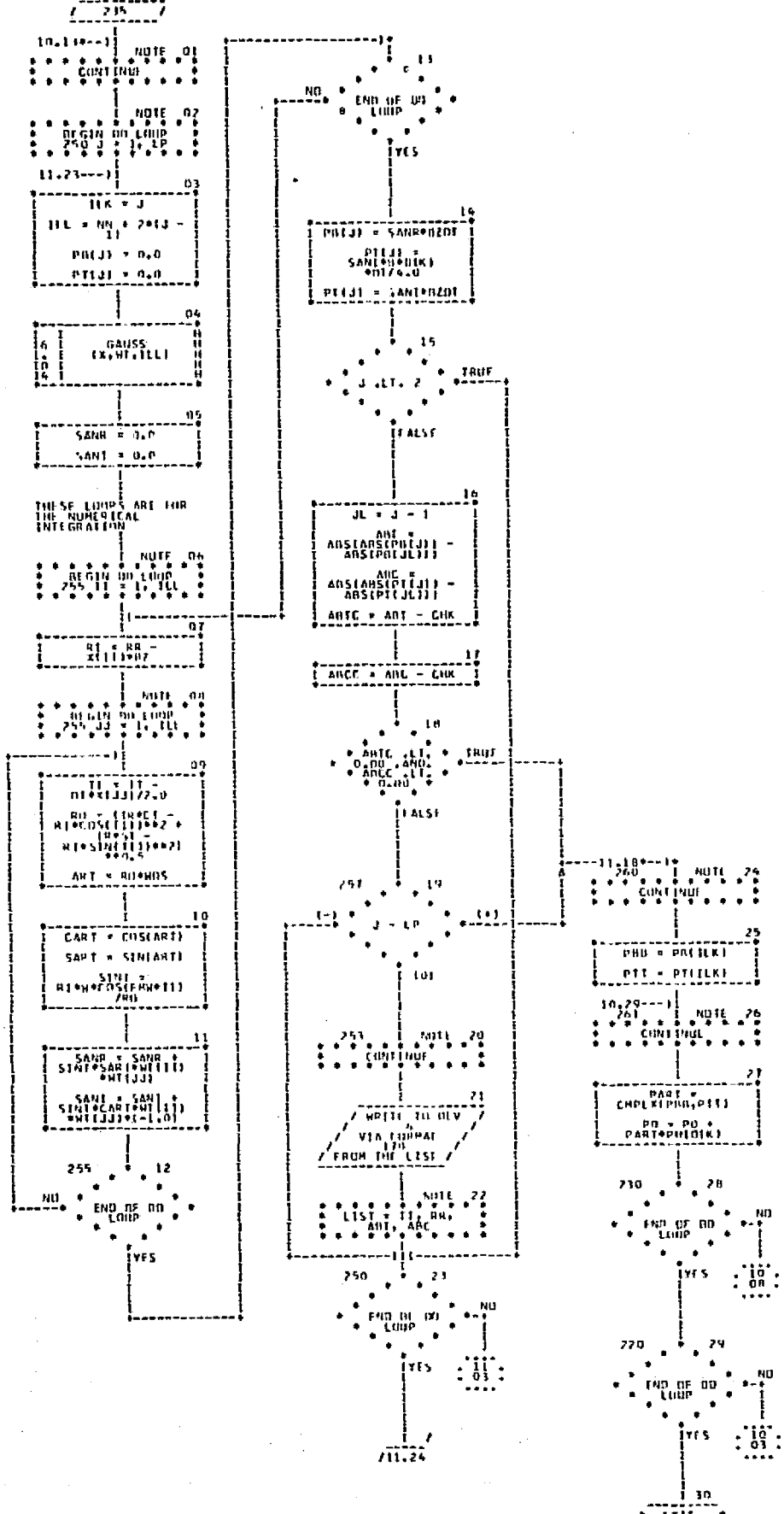
**PRECEDING PAGE BLANK NOT FILMED**



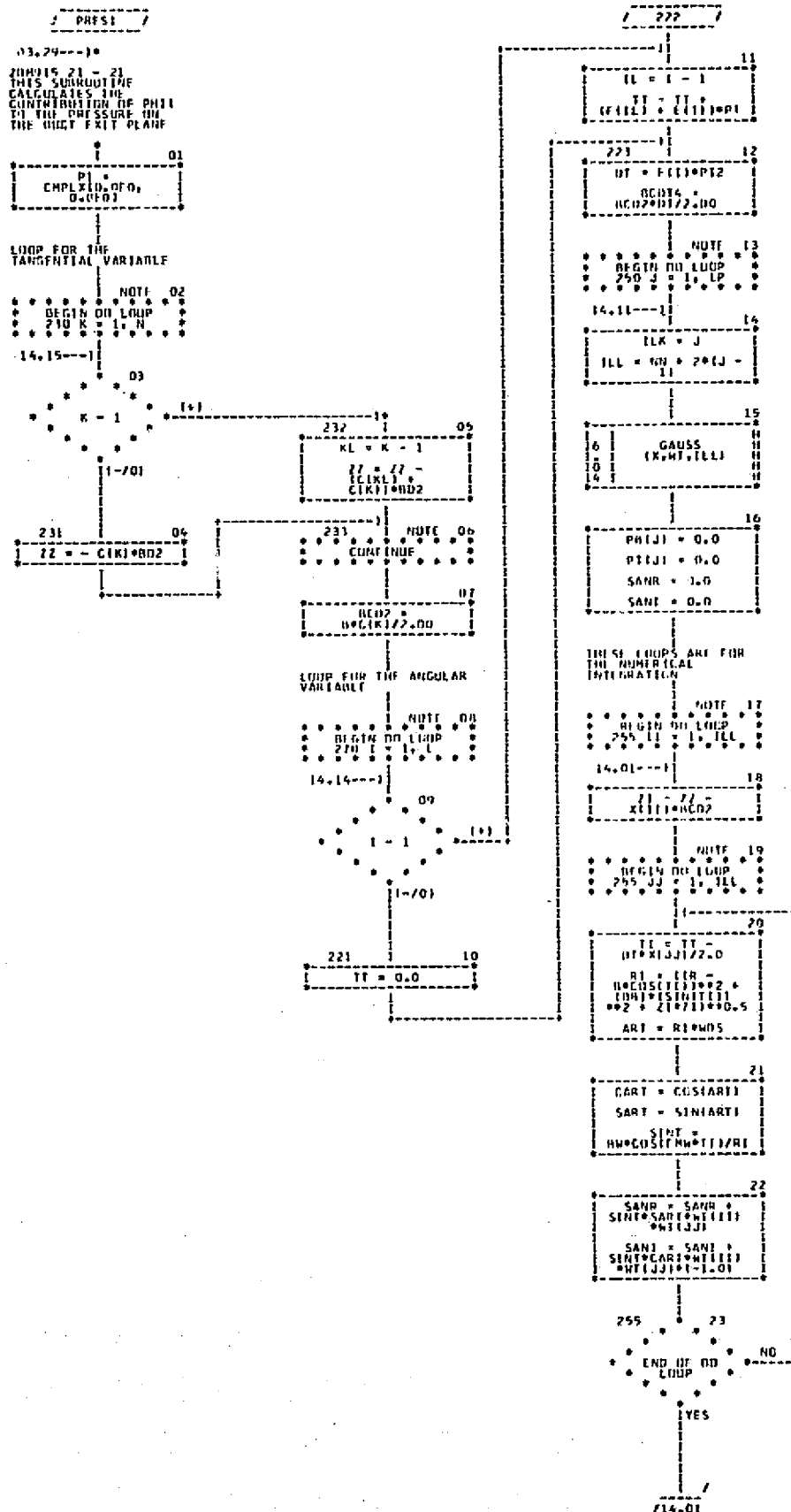


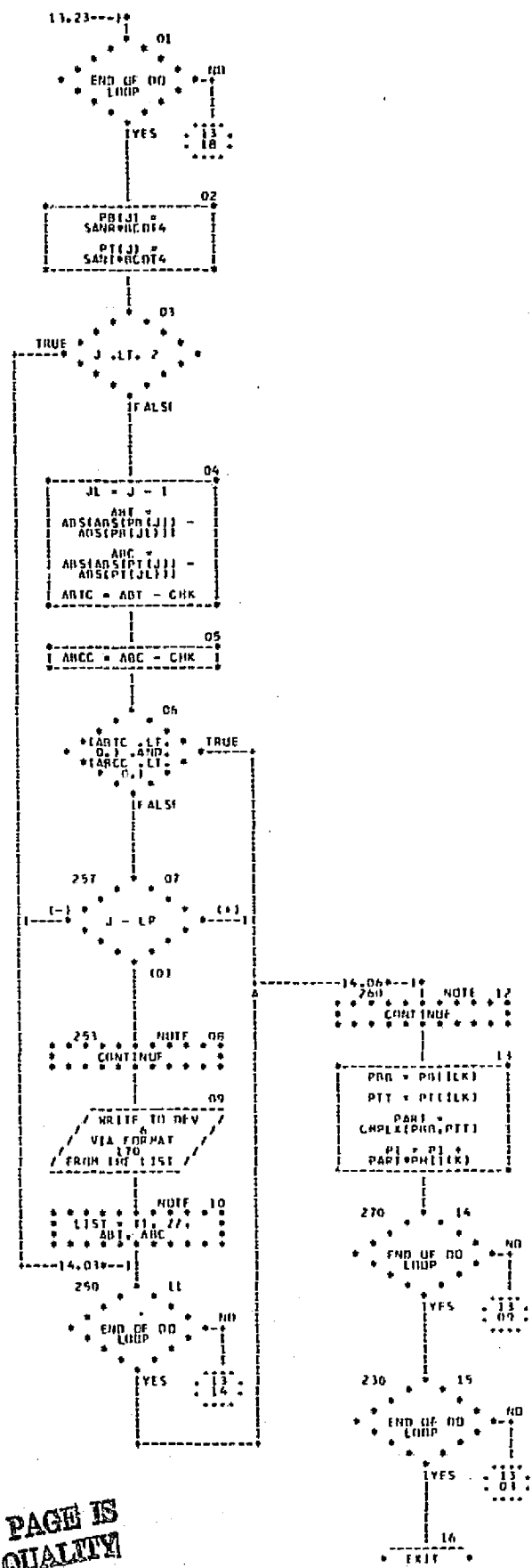
ORIGINAL PAGE IS  
OF POOR QUALITY





ORIGINAL PAGE IS  
 OF POOR QUALITY

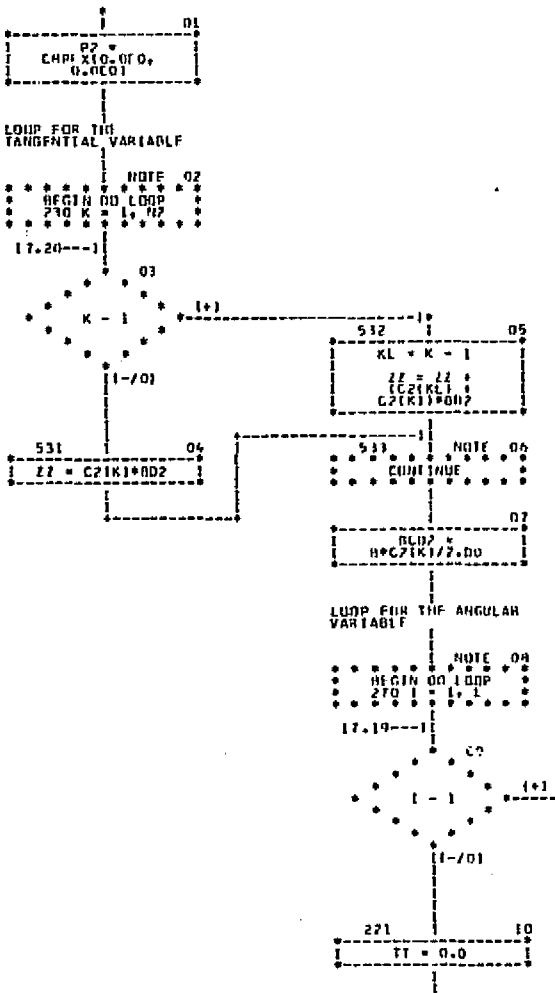




/ PRES2 /

03.31-->1\*

DIM015 71  
INPUT SUBROUTINE  
CALCULATES THE  
CONTRIBUTION OF PHIZ  
TO THE PRESSURE ON  
THE DUCT EXIT PLATE



/ 222 /

11 ILL = 1 - 1

12 IF(I11 < 1) GOTO1

13 223 DE = 1.0/(PP12)

DIM015 =  
B\*D(I11)\*DE/4.00

14 WRITE TO DEV

VIA EDIFAT

FROM THE LIST

15 NOTE

\* \* \* LIST \* \* \* 22 \* \* \*

16 NOTE 15

\* \* \* BEGIN DO LOOP \* \* \*

270 J = 1, N1

17.13--->1

17 WRITE TO DEV

VIA EDIFAT

FROM THE LIST

18 NOTE

\* \* \* LIST \* \* \* J \* \* \*

19 ILL = J

ILL = NN + 2\*I11 - 1

PR1JJ = 0.0

PT1JJ = 0.0

20 GAUSS

(X,WT,ILL)

21 SANR = 0.0

SANI = 0.0

22 THESE LOOPS ARE FOR

THE NUMERICAL

INTEGRATION

23 NOTE

\* \* \* BEGIN DO LOOP \* \* \*

270 JJ = 1, ILL

17.01--->1

24 21 ILL = JJ - 1

RT1 = 4\*IR -

ARCSIN((1+I11)/2.0)

ARCSIN((1-I11)/2.0)

ART = RT1\*WDS

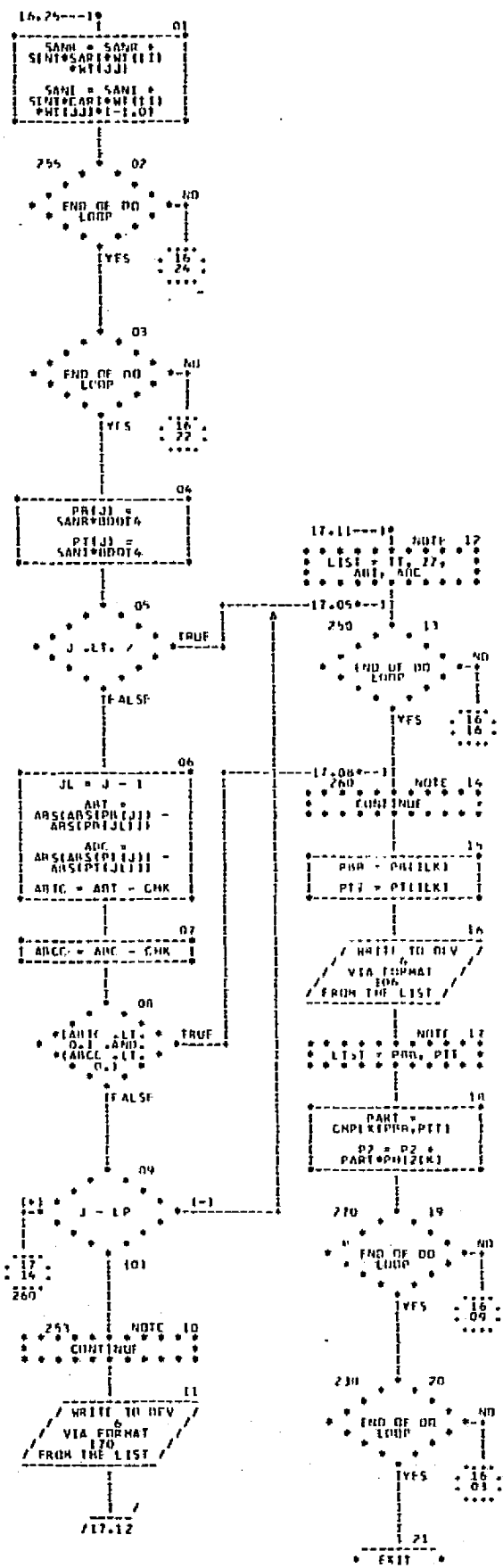
25 CART = COS(ART)

SART = SIN(ART)

SINT =

AMPCOS(WDS\*ART)

/17.01

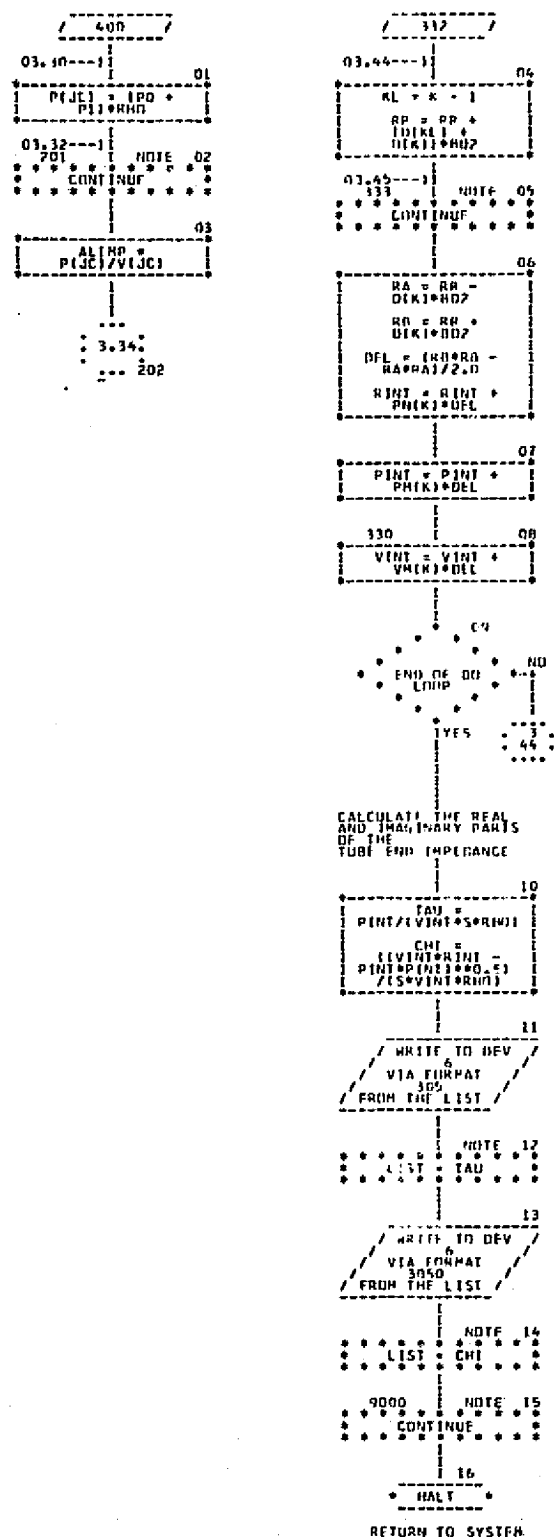


ORIGINAL PAGE IS  
OF POOR QUALITY

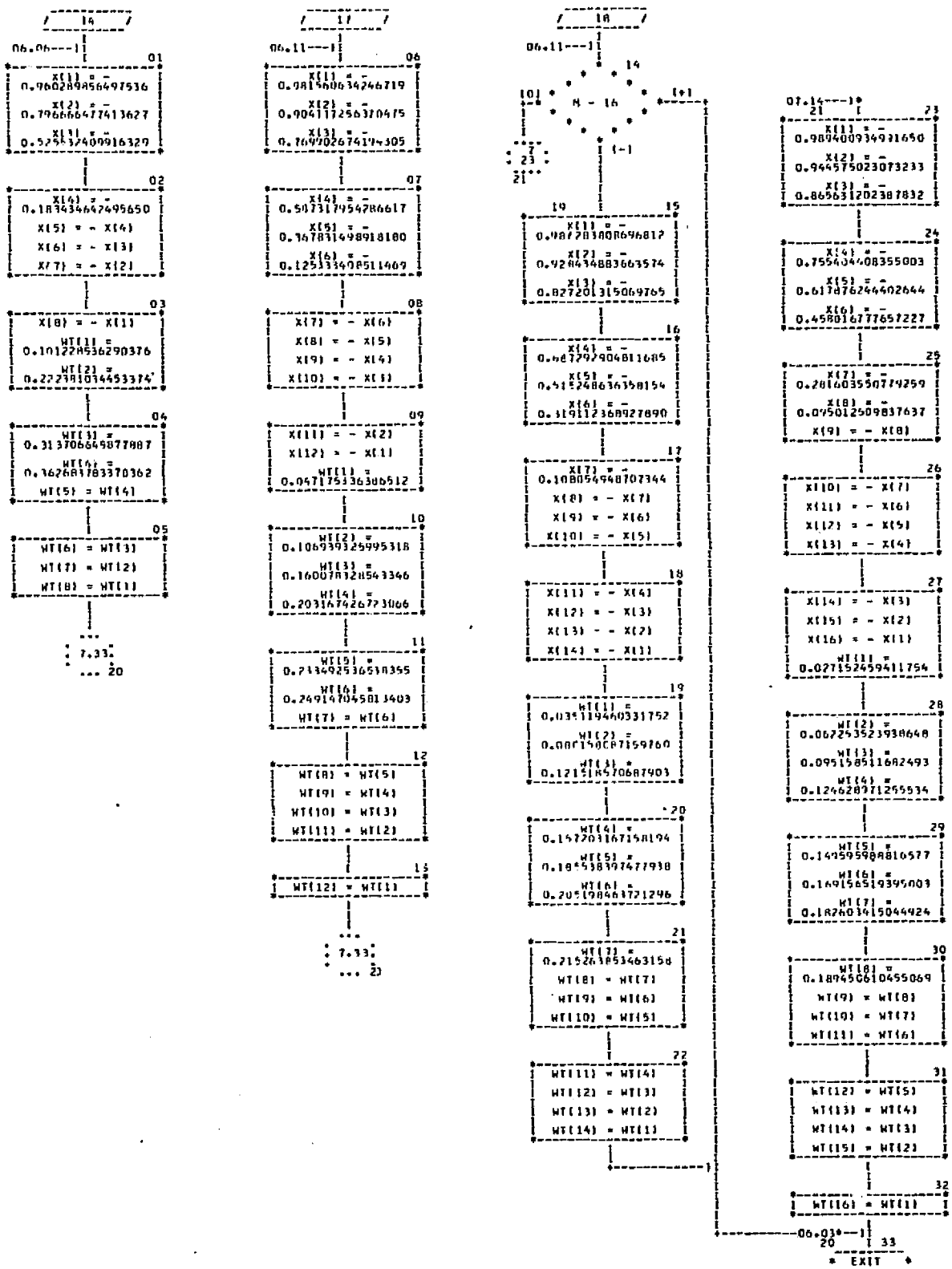
```

/ GAUSS /
11.049--1
    04
    (01) * H = 4 [+]
11   01
X(11) = 0.86111611594053
X(21) = 0.339981043584856
X(31) = - X(21)
12   06
    01
    (01) * H = 8 [+]
12   01
X(12) = 0.517350269109626
X(21) = X(11)
WT(11) = 1.0
WT(21) = 1.0
13   07
    01
    (01) * H = 12 [+]
13   01
X(13) = 0.912469514203152
X(21) = 0.661209388466265
X(31) = 0.238619186083197
14   08
    01
    (01) * H = 16 [+]
14   01
X(14) = - X(31)
X(21) = - X(21)
X(31) = - X(11)
WT(11) = 0.171324492379170
15   11
    01
    (01) * H = 12 [+]
15   01
X(15) = 0.973906528517172
X(21) = - 0.8650033668985
X(31) = - 0.679409568299024
16   12
    01
    (01) * H = 13 [+]
16   01
X(16) = 0.433195194129247
X(21) = 0.148874338981631
X(31) = - X(51)
17   13
    01
    (01) * H = 14 [+]
17   01
X(17) = - X(61)
X(21) = - X(31)
X(31) = - X(21)
X(10) = - X(11)
18   14
    01
    (01) * H = 15 [+]
18   01
WT(11) = 0.066671346308688
WT(21) = 0.149451349150581
WT(31) = 0.214086362515982
19   15
    01
    (01) * H = 16 [+]
19   01
WT(11) = WT(41)
WT(21) = WT(31)
WT(31) = WT(21)
WT(10) = WT(11)
20   16
    01
    (01) * H = 17 [+]
20   01
X(17) = - X(61)
X(21) = - X(31)
X(31) = - X(21)
X(10) = - X(11)
21   17
    01
    (01) * H = 18 [+]
21   01
WT(11) = WT(41)
WT(21) = WT(31)
WT(31) = WT(21)
WT(10) = WT(11)
22   18
    01
    (01) * H = 19 [+]
22   01
X(17) = - X(61)
X(21) = - X(31)
X(31) = - X(21)
X(10) = - X(11)

```



ORIGINAL PAGE IS  
OF POOR QUALITY



**APPENDIX 3**

**MAIN PROGRAM LISTING**

C THIS PROGRAM CALCULATES THE ACOUSTIC IMPEDANCE OF  
C THE DUCT EXIT PLANE

ZDM915 20 - 20

INTEGER \*4 DRECTP /02/  
COMPLEX \*8 CMPLX  
1 ,PO,P1,P2,P  
2 ,PHIO(40), PHI1(40),PHI2(40) ,V(40),ALIMP  
DIMENSION  
1 PN(40),PD(2,1) ,VD(2,1) ,VM(40),PM(40)  
2 ,D(40),C(40),P(80) ,C2(40) ,E(40)  
EQUIVALENCE (PD(1,1),P(1)) ,(VD(1,1),V(1))  
COMMON/EATA/L,M,N,NN,LP,MW,A,B,W,S,CHK,D,C,E,PI  
COMMON/PHI/PHIO,PHI1,PHI2,PO,P1,P2  
COMMON /C2N2/ C2,N2  
COMMON/ANG/ FINK, BD2, WDS, FMW, PI2, BW, AW ,BB,AA  
100 FORMAT (36I2)  
220 FORMAT (6E12.5)  
1000 FORMAT ('1 TUBE END IMPEDANCE PROGRAM FOR UNFLANGED ANNULAR DUCT  
1.'// 25X, 'I N P U T D A T A')  
402 FORMAT ('0 THETA BOX WIDTH ON DUCT FACE')  
403 FORMAT ('1 VELOCITY ON DUCT FACE')  
407 FORMAT ('1')  
408 FORMAT ('0 A =', 1PE13.6, ' B =', E13.6, ' W =', E13.6, ' S =',  
1 E13.6/ 'OCHK=', E13.6, ' RHO=', E13.6)  
1100 FORMAT ('0 ANNULAR RING BOX WIDTHS' /)  
1200 FORMAT ('0 OUTER DUCT WALL BOX LENGTHS' /)  
1300 FORMAT ('0 INNER DUCT WALL BOX LENGTHS' /)  
1400 FORMAT ('0 SOURCE DISTRIBUTION ON DUCT FACE.' /)  
1500 FORMAT ('0 SOURCE DISTRIBUTION ON OUTER DUCT WALL' /)  
1600 FORMAT ('0 SOURCE DISTRIBUTION ON INNER DUCT WALL' /)  
C \*  
READ (5,100) K, M, N, N2, INK, MW, NN, L,LP  
RFAD (5,220) A, B, W, S, CHK, XANG , RHO  
READ (5,220) (C(I), I=1,N)  
READ (5,220) (D(I), I=1,M)  
IF (INK .GT. 0) READ (5,220) (C2(I),I=1,N2)  
READ (5,220) (V(I), I=1,M)  
READ (5,220) (PHIO(I),I=1,M)  
READ (5,220) (PHI1(I),I=1,N)  
IF (INK .GT. C) READ (5,220) (PHI2(I),I=1,N2)  
E(1) = XANG  
DT2= (1.0E0 - XANG) / (L-1)  
DO 50 I=2,L  
50 F(I) = DT2  
105 FORMAT (1PE16.6, 3E18.6)  
104 FORMAT ('C L =', I4, ' M =', I4, ' N =', I4, ' NN =', I4,  
1 ' LP =', I4, ' MW =', I5, ' INK =', I5/)  
WRITE (6,1000)  
WRITE(6,408) A,B,W,S,CHK, RHO  
WRITE(6,104) L,M,N,NN,LP,MW,INK  
WRITE(6,105) (D(I),I=1,M)

```

      WRITE (6, 1200)
      WRITE(6,105) (C(I),I=1,N)
      IF (INK .GT. 0) WRITE (6, 1300)
      IF (INK .GT. 0) WRITE (6, 105) (C2(I), I = 1,N)
      WRITE (6, 402)
      WRITE(6,105) (E(I),I=1,L)
      WRITE (6, 403)
      WRITE(6,105) (V(I),I=1,M)
      WRITE (6, 1400)
      WRITE(6,105) (PHIO(I),I=1,M)
      WRITE (6, 1500)
      WRITE(6,105) (PHI1(I),I=1,N)
      IF (INK .GT. 0)      WRITE (6, 1600)
      IF (INK .GT. 0)      WRITE (6,105) (PHI2(I),I=1,N2)
      C**          INITIALIZATION *   *   *   *   *
      PI=3.141592653589793
      FINK = FLOAT(INK)
      BD2 = B / 2.0D0
      WDS = W / S
      FMW = FLOAT(MW)
      PI2 = PI * 2.0D0
      BH = B * H
      AW = A * W
      AA = A * A
      BB = B * B
      C
      C          THIS LOOP CALCULATES THE RADIAL PRESSURE DISTRIBUTION
      C
      DO 200 JC=1,M
      P(JC)= CMPLX(0.0E0,0.0E0)
      IF(JC-1)210,210,211
      210 R=D(JC)*BD2 +A* FINK
      GO TO 212
      211 JE=JC-1
      R=R+(D(JE)+D(JC))*BD2
      212 CONTINUE
      IF (R.GT.A)          GO TO 170
      IF (INK.EQ.1 .OR. VD(1,JC).EQ.0.D0)          GO TO 203
      151 FORMAT(1HC,5X,I3,6X,D25.14)
      170 CONTINUE
      CALL PRES0(R)
      CALL PRES1(R)
      IF(INK-1) 400,500,500
      500 CALL PRES2(R)
      P(JC)= (P0 + P1 + P2) * RHO
      GO TO 201
      400 P(JC) = (P0 + P1) * RHO
      201 CONTINUE
      ALIMP = P(JC) / V(JC)
      GO TO 202
      203 P(JC)= CMPLX(0.0E0,0.0E0)

```

```

202 CONTINUE
  WRITE(6, 160) JC, R, ALIMP, P(JC), V(JC)
160 FORMAT (' ANNULAR RING NO', I3, ' RADIAL POSITION =', 1PE14.6/
     1      25X, 'LOCAL IMPEDANCE =', 2E14.6/
     2      32X, 'PRESSURE =', 2E14.6/
     3      32X, 'VELOCITY =', 2E14.6/)

200 CONTINUE
C
C       THIS LOOP INTEGRATES THE VELOCITY AND PRESSURE DISTRIBUTIONS
C       OVER THE DUCT FACE
C
  DO 300 I=1,M
    VM(I)=VD(1,I)**2+VD(2,I)**2
    PN(I)=PD(1,I)**2+PD(2,I)**2
300 PM(I)=PD(1,I)*VD(1,I) + PD(2,I) * VD(2,I)
    RINT=0.C
    PINT=0.C
    VINT=0.C
    DO 330 K=1,M
      IF (K-1) 331,331,332
331 RR=D(K)*BD2 + FINK * A
      GO TO 333
332 KL=K-1
    RR=RR+(D(KL)+D(K))*BD2
333 CONTINUE
    RA=RR-D(K)*BD2
    RR=RR+D(K)*BD2
    DEL=(RB*RB-RA*RA)/2.0
    RINT=RINT+PN(K)*DEL
    PINT=PINT+PM(K)*DFL
    330 VINT=VINT+VM(K)*DEL

C
C       CALCULATE THE REAL AND IMAGINARY PARTS OF THE
C       TUBE END IMPEDANCE
C
    TAU=PINT/(VINT*S*RHO)
    CHI=((VINT*RINT-PINT*PINT)**0.5)/(S*VINT*RHO)
    WRITE(6,305) TAU
305 FORMAT(1H ,10X,'RESISTANCE RATIO, TAU = ',E15.8)
    WRITE(6,3050) CHI
3050 FORMAT(1H ,10X,'REFRACTANCE RATIO, CHI = ',E15.8)
9000 CONTINUE
    STOP
    END

```

**APPENDIX 4**

**PRESO SUBROUTINE LISTING**

## SUBROUTINE PRESC(R)

ZDM915 21 - 21

```

C      THIS SURROUTINE CALCULATES THE CONTRIBUTION OF PHI0
C      TO THE PRESSURE ON THE DUCT EXIT PLANE
REAL *4 F5D8/.625D0/, F5D12/.416666666666666D0/
1 ,F16D5 /3.2D0/ ,F6D5/1.2D0/
COMPLEX *8 CMPLX
1           ,PHI0(40), PHI1(40), PHI2(40), P0, P1, P2, PART
DIMENSION X(20),WT(20),D(40),C(40),E(40),PB(40),PT(40)
COMMON/PHI/PHI0,PHI1,PHI2,P0,P1,P2
COMMON/DATA/L,M,N,NN,LP,MW,A,B,W,S,CHK,D,C,E,PI
COMMON/ANG/   FINK, BD2, WDS, FMW, PT2, BW, AW, RB, AA
PO= CMPLX(0.0E0,0.0E0)
CT=1.0
ST=0.0

```

## LOOP FOR THE ANGULAR VARIABLE

```

DO 220 KC=1,L
IF(KC-1)221,221,222
221 TT=0.0
GO TO 223
222 KCL=KC-1
TT=TT+(E(KCL)*E(KC))*PI
223 DT=E(KC)*2.0*PI

```

## LOOP FOR THE RADIAL VARIABLE

```

DO 230 K=1,M
IF(K-1)231,231,232
231 RR=D(K)*BD2 +A* FINK
GO TO 233
232 KL=K-1
RR=RR+(D(KL)+D(K))*BD2
233 CONTINUE

```

## CLOSED FORM INTEGRATION OVER THE PRESSURE SINGULARITY

```

BZ=D(K)*BD2
AZ=R*DT/2.0
BZDT = BZ * DT / 2.0D0
IF(KC-1)234,234,235
234 RQ=R+D(K)*B/5.0
RP=R-D(K)*B/5.0
IF((RR.GE.RQ).OR.(RR.LE.RP)) GO TO 235
TN=BZ/AZ
ALP=ATAN(TN)
SEC=1.0/ COS(ALP)
SEC2 = SEC * SFC
SEC4 = SEC2 * SEC2
SEC6 = SEC4 * SEC2

```

```

CSC=1.0/ SIN(ALP)
CSC2 = CSC * CSC
CSC4 = CSC2 * CSC2
CSC6 = CSC4 * CSC2
COT=1.0/TN
CF1=AZ*ALOG(( SEC+TN)/( SEC-TN))*W*(-2.0)
WA=W*AZ/S
WA2 = WA * WA
WA4 = WA2 * WA2
WA6 = WA4 * WA2
CF1=CF1*(1.0-WA2 /12.0+WA4 /320.0- WA6 /16128.0)
CF2=WA2 *W*AZ*TN*SEC/3.0
CF2=CF2*(1.0-WA2 *(SEC2 +1.5)/40.0+WA4 *(SEC4 /3.0+ SEC2
1*F5D12+ F5D8 )/840.0)
CF3=BZ*ALOG(( CSC+COT)/( CSC-COT))*W*(-2.0)
WB=W*BZ/S
WB2 = WB * WB
WB4 = WB2 * WB2
WB6 = WB4 * WB2
CF3=CF3*(1.0-WB2 /12.0+WB4 /320.0-WB6 /16128.0)
CF4=WB2 *W*BZ*COT*CSC/3.0
CF4=CF4*(1.0-WB2 *(CSC2 +1.5)/40.0+WB4 *(CSC4 /3.0+ CSC2
1*F5D12 + F5D8 )/840.0)
PTT=CF1+CF2+CF3+CF4
DF1=WA2 *S*TN*2.0
DF1=CF1*(1.0-WA2 *(SEC2 +2.0)/36.0+WA4 *(3.0*SEC4 +4.0*SEC2
1+8.0)/5400.0-WA6 *(15.0*SEC6 +18.0*SFC4 +24.0*SFC2 +48.0)/2116
2800.0)
DF2=WB2 *S*COT*2.0
DF2=DF2*(1.0-WB2 *(CSC2 +2.0)/36.0+WB4 *(3.0*CSC4 +4.0*CSC2 +
18.0)/5400.0-WB6 *(CSC6 +6.0*CSC4 /5.0+8.0*CSC2 /5.0+F16D5 )/
2141120.C)
PBR=DF1+DF2
GO TO 261
235 CONTINUE
DO 250 J=1,LP
ILK=J
ILL=NN+2*(J-1)
PB(J)=0.C
PT(J)=0.C
CALL GAUSS(X,WT,ILL)
SANR=0.C
SANI=0.C
C
C      THESE LOOPS ARE FOR THE NUMERICAL INTEGRATION
C
DO 255 II=1,ILL
RI=RR- X(II) * BZ
DO 255 JJ=1,ILL
TI=TT-DT*X(JJ)/2.0
RJ=((R*CT-RI* COS(TI))**2+(R*ST-RI* SIN(TI))**2)**0.5

```

```

ART=RO*WDS
CART= COS(ART)
SART= SIN(ART)
SINT=R1*W* COS( FMW      *T1)/RO
SANR=SANR+SINT*SART*WT(I1)*WT(JJ)
SANI=SANI+SINT*CART*WT(I1)*WT(JJ)*(-1.0)
255 CONTINUE
PB(J)=SANR*BZDT
PT(J)=SANI*B*D(K)*DT/4.0
PT(J)=SANI*BZDT
IF (J .LT. 2)                                GO TO 250
JL=J-1
ABT= ABS( ABS(PB(J))- ABS(PB(JL)))
ABC= ABS( ABS(PT(J))- ABS(PT(JL)))
ABTC=ABT-CHK
ABCC=ABC-CHK
IF (ABTC.LT.0.00 .AND. ABCC.LT.0.00)        GO TO 260
257 IF(J-LP) 250,253,260
253 CONTINUE
WRITE (6,170) TT,RR,ABT,ABC
170 FORMAT(1HO,  'INTEGRATION FOR BLOCK CENTERED AT THETA=',1PE13.6,
1' R=', E13.6 ,/,19X,'DID NOT CONVERGE',/,19X,'REAL DIFF =',E13.6
2 , ' IMAG DIFF = ',E13.6)
250 CONTINUE
260 CONTINUE
PBB=PB(ILK)
PTT=PT(ILK)
261 CONTINUE
PART= CMPLX(PBB,PTT)
PO=PO+PART*PHIO(K)
230 CONTINUE
220 CONTINUE
RETURN
END

```

## **APPENDIX 5**

### **PRES1 SUBROUTINE LISTING**

SUBROUTINE PRES1(R)

ZDM915 21 - 21

C THIS SUBROUTINE CALCULATES THE CONTRIBUTION OF PHI1  
C TO THE PRESSURE ON THE DUCT EXIT PLANE  
C COMPLEX \*8 CMPLX  
1 ,PHIO(40), PHI1(40), PHI2(40), P0, P1, P2, PART  
DIMENSION X(20),WT(20),D(40),C(40),F(40),PR(40),PT(40)  
COMMON/CATA/L,M,N,NN,LP,MW,A,B,W,S,CHK,D,C,E,PI  
COMMON/PHI/PHIO,PHI1,PHI2,P0,P1,P2  
COMMON/ANG/ FINK, BD2, WDS, FMW, PI2, BW, AW,BB, AA  
P1= CMPLX(C,OFO,C,OEO)

C LOOP FOR THE TANGENTIAL VARIABLE

DO 230 K=1,N  
IF(K-1) 231,231,232  
231 ZZ=-C(K)\*BD2  
GO TO 233  
232 KL=K-1  
ZZ=ZZ-(C(KL)+C(K))\*BD2  
233 CONTINUE  
BCD2 = B \* C(K) / 2.D0

C LOOP FOR THE ANGULAR VARIABLE

DO 270 I=1,L  
IF(I-1) 221,221,222  
221 TT=0.0  
GO TO 223  
222 IL=I-1  
TT=TT+(E(IL)+E(I))\*PI  
223 DT=E(I)\* PI2  
BCDT4 = BCD2 \* DT / 2.D0  
DO 250 J=1,LP  
ILK=J  
ILL=NN+2\*(J-1)  
CALL GAUSS(X,WT,ILL)  
PB(J)=0.C  
PT(J)=C.C  
SANR=0.C  
SANI=0.C

C THESE LOOPS ARE FOR THE NUMERICAL INTEGRATION

DO 255 II=1,ILL  
ZI=ZZ- X(II) \* BCD2  
DO 255 JJ=1,ILL  
TI=TT-DT\*X(JJ)/2.0  
RT=((R-B\* COS(TI))\*\*2+(BB )\*( SIN(TI))\*\*2+ZI\*ZI)\*\*0.5  
ART=RI\*DCS  
CART= CCS(ART)

```

SART= SIN(ART)
SINT=BW * COS( FMW      *YI)/RI
SANR=SANR+SINT*SART*WT(IJ)*WT(JJ)
SANI=SANI+SINT*CART*WT(IJ)*WT(JJ)*(-1.0)
255 CONTINUE
PB (J)=SANR*BCDT4
PT (J)=SANI*BCDT4
  IF (J .LT. 2)                               GO TO 250
  JL=J-1
  ABT= ABS( ABS(PB(J))- ABS(PB(JL)))
  ABC= ABS( ABS(PT(J))- ABS(PT(JL)))
  ABTC=ABT-CHK
  ABCC=ABC-CHK
  IF((ABTC.LT.0.) .AND. (ABCC.LT.0.)) GO TO 260
257 IF(J-LP) 250,253,260
253 CONTINUE
  WRITE (6,170) TT,ZZ,ABT,ABC
170 FORMAT(1HO,    'INTEGRATION FOR BLOCK CENTERED AT THETA=',1PE13.6,
     1' Z=', E13.6 ,/,19X,'DID NOT CONVERGE',/,19X,'REAL DIFF =',E13.6
     2 , ' IMAG DIFF = ',E13.6)
250 CONTINUE
260 CONTINUE
  PBB=PB(ILK)
  PTT=PT(ILK)
  PART= CMPLX(PBB,PTT)
  P1=P1+PART*PHI1(K)
270 CONTINUE
230 CONTINUE
  RETURN
END

```

## **APPENDIX 6**

### **PRES2 SUBROUTINE LISTING**

**PRECEDING PAGE BLANK NOT FILMED**

SUBROUTINE PRES2(R)

ZDM915 21 - 21

C THIS SUBROUTINE CALCULATES THE CONTRIBUTION OF PHI2  
C TO THE PRESSURE ON THE DUCT EXIT PLANE

COMPLEX \*8 CMPLX

COMPLEX \*8 PHI0(40), PHI1(40), PHI2(40), P0, P1, P2, PART

DIMENSION X(20), WT(20), D(40), C(40), E(40), PB(40), PT(40), C2(40)

COMMON/PHI/PHIC, PHI1, PHI2, P0, P1, P2

COMMON/DATA/L, M, N, NN, LP, MW, A, B, W, S, CHK, D, C, E, PI

COMMON/C2N2/C2, N2

COMMON/ANG/ FINK, BD2, WDS, FMW, PI2, BW, AW, BB, AA

P2= CMPLX(0.0E0,0.0E0)

105 FORMAT(1H ,2X,4D25.14)

C LOOP FOR THE TANGENTIAL VARIABLE

DO 230 K=1,N2

IF(K-1)531,531,532

531 ZZ=C2(K)\*BD2

GO TO 533

532 KL=K-1

ZZ=ZZ+(C2(KL)+C2(K))\*BD2

533 CONTINUE

C BCD2 = B \*C2(K) / 2.D0

C LOOP FOR THE ANGULAR VARIABLE

DO 270 I=1,L

IF(I-1) 271,221,222

221 TT=0.0

GO TO 223

222 IL=I-1

TT=TT+(F(IL)+E(I))\*PI

223 DT=E(I)\* PI2

BDDT4 = B \* D(K) \* DT / 4.D0

WRITE(6,105) TT,ZZ

DO 250 J=1,LP

WRITE(6,5) J

5 FORMAT(1H ,10X,[5])

ILK=J

ILL=NN+2\*(J-1)

PB(J)=0.0

PT(J)=0.0

CALL GALSS(X,WT,ILL)

SANR=0.0

SANI=0.0

C THESE LOOPS ARE FOR THE NUMERICAL INTEGRATION

DO 255 II=1,ILL

ZI=ZZ- X(II) \* BCD2

```

DO 255 JJ=1,ILL
TI=TT-DT*X(JJ)/2.0
RI=((R-A*COS(TI))**2+AA*(SIN(TI))**2+ZI*ZI)**0.5
ART=RI*WCS
CART=COS(ART)
SART=SIN(ART)
SINT=AW*COS(FMW*TI)/RI
SANR=SANR+SINT*SART*WT(I)*WT(JJ)
SANI=SANI+SINT*CART*WT(I)*WT(JJ)*(-1.0)
255 CONTINUE
PB(J)=SANR*BDDT4
PT(J)=SANI*BDDT4
IF (J .LT. 2) GO TO 250
JL=J-1
ABT= ABS(ABS(PB(J))-ABS(PB(JL)))
ABC= ABS(ABS(PT(J))-ABS(PT(JL)))
ABTC=ABT-CHK
ABCC=ABC-CHK
IF((ABTC.LT.0.) .AND. (ABCC.LT.0.)) GO TO 260
IF(J-LP) 250,253,260
253 CONTINUE
WRITE(6,170) TT,ZZ,ABT,ABC
170 FORMAT(1H0, 'INTEGRATION FOR BLOCK CENTERED AT THETA=',1PE13.6,
1' Z=', E13.6 ,/,19X,'DID NOT CONVERGE',/,19X,'REAL DIFF =',E13.6
2 , ' IMAG DIFF = ',E13.6)
250 CONTINUE
260 CONTINUE
PBB=PB(ILK)
PTT=PT(ILK)
WRITE(6,106) PBB,PTT
106 FORMAT(1H ,10X,'P2 REAL =',E25.7 , ' P2 IMAG=',E25.7 /)
PART= CMPLX(PBB,PTT)
P2=P2+PART*PHI2(K)
270 CONTINUE
230 CONTINUE
RETURN
END

```

**APPENDIX 7**

**GAUSS SUBROUTINE LISTING**

**PRECEDING PAGE BLANK NOT FILMED**

```

SUBROUTINE GAUSS(X,WT,M)
DIMENSION X(12),WT(12)
IF(M=4)10,11,12
10 X(1)=-0.577350269189626
X(2)=-X(1)
WT(1)=1.0
WT(2)=1.0
GO TO 20
11 X(1)=-0.861136311594053
X(2)=-0.339981043584856
X(3)=-X(2)
X(4)=-X(1)
WT(1)=0.347854845137454
WT(2)=0.652145154862546
WT(3)=WT(2)
WT(4)=WT(1)
GO TO 20
12 IF(M=8)13,14,15
13 X(1)=-0.932469514203152
X(2)=-0.661209386466265
X(3)=-0.238619186083197
X(4)=-X(3)
X(5)=-X(2)
X(6)=-X(1)
WT(1)=0.171324492379170
WT(2)=0.360761573048139
WT(3)=0.467913934572691
WT(4)=WT(3)
WT(5)=WT(2)
WT(6)=WT(1)
GO TO 20
14 X(1)=-0.960289856497536
X(2)=-0.796666477413627
X(3)=-0.525532409916329
X(4)=-0.183434642495650
X(5)=-X(4)
X(6)=-X(3)
X(7)=-X(2)
X(8)=-X(1)
WT(1)=0.101228536290376
WT(2)=0.222381034453374
WT(3)=0.313706645877887
WT(4)=0.362683783378362
WT(5)=WT(4)
WT(6)=WT(3)
WT(7)=WT(2)
WT(8)=WT(1)
GO TO 20
15 IF(M=12)16,17,18
16 X(1)=-0.973906528517172
X(2)=-0.865063366688985

```

```

X{3}=-0.679409568299024
X{4}=-0.433395394129247
X{5}=-0.148874338981631
X{6}=- X{5}
X{7}=- X{4}
X{8}=- X{3}
X{9}=- X{2}
X{10}=- X{1}
WT{1}=0.066671344308688
WT{2}=0.149451349150581
WT{3}=0.219086362515982
WT{4}=0.269266719309996
WT{5}=0.295524224714753
WT{6}=WT{5}
WT{7}=WT{4}
WT{8}=WT{3}
WT{9}=WT{2}
WT{10}=WT{1}
GO TO 20
17 X{1}=-0.981560634246719
X{2}=-0.904117256370475
X{3}=-0.769902674194305
X{4}=-0.587317954286617
X{5}=-0.367831498918180
X{6}=-0.125333408511469
X{7}=- X{6}
X{8}=- X{5}
X{9}=- X{4}
X{10}=- X{3}
X{11}=- X{2}
X{12}=- X{1}
WT{1}=0.047175336386512
WT{2}=0.106939325995318
WT{3}=0.160078328543346
WT{4}=0.203167426723066
WT{5}=0.233492536538355
WT{6}=0.249147045813403
WT{7}=WT{6}
WT{8}=WT{5}
WT{9}=WT{4}
WT{10}=WT{3}
WT{11}=WT{2}
WT{12}=WT{1}
GO TO 20
18 IF (M=16)
19 X{1}=-0.986283808696812
X{2}=-0.928434883663574
X{3}=-0.827201315069765
X{4}=-0.687292904811685
X{5}=-0.515248636358154
X{6}=-0.319112368927890
19, 21, 20

```

```

X{ 7}=-0.108054948707344
X{ 8}=- X{ 7}
X{ 9}=- X{ 6}
X{10}=- X{ 5}
X{11}=- X{ 4}
X{12}=- X{ 3}
X{13}=- X{ 2}
X{14}=- X{ 1}
WT{ 1}=0.035119460331752
WT{ 2}=0.080158087159760
WT{ 3}=0.121518570687903
WT{ 4}=0.157203167158194
WT{ 5}=0.185538397477938
WT{ 6}=0.205198463721296
WT{ 7}=0.215263853463158
WT{ 8}=WT{ 7}
WT{ 9}=WT{ 6}
WT{10}=WT{ 5}
WT{11}=WT{ 4}
WT{12}=WT{ 3}
WT{13}=WT{ 2}
WT{14}=WT{ 1}

```

GO TO 20

```

21 X{ 1}=-0.989400934991650
X{ 2}=-0.944575023073233
X{ 3}=-0.865631202387832
X{ 4}=-0.755404408355003
X{ 5}=-0.617876244402644
X{ 6}=-0.458016777657227
X{ 7}=-0.281603550779259
X{ 8}=-0.095012509837637
X{ 9}=- X{ 8}
X{10}=- X{ 7}
X{11}=- X{ 6}
X{12}=- X{ 5}
X{13}=- X{ 4}
X{14}=- X{ 3}
X{15}=- X{ 2}
X{16}=- X{ 1}
WT{ 1}=0.027152459411754
WT{ 2}=0.062253523938648
WT{ 3}=0.095158511682493
WT{ 4}=0.124628971255534
WT{ 5}=0.149595988816577
WT{ 6}=0.169156519395003
WT{ 7}=0.182603415044924
WT{ 8}=0.189450610455069
WT{ 9}=WT{ 8}
WT{10}=WT{ 7}
WT{11}=WT{ 6}
WT{12}=WT{ 5}

```

WT(13)=WT(4)  
WT(14)=WT(3)  
WT(15)=WT(2)  
WT(16)=WT(1)

20 RETURN  
END

## **APPENDIX 8**

### **EXAMPLE PROBLEM**

**PRECEDING PAGE BLANK NOT FILMED**

001640000C000C 23C 8

1.C 343.0 343.0 .0001 .03

1.21

2.50000D-02 2.50000D-02 5.00000D-02 5.00000D-02 5.00000D-02 5.00000D-02  
7.50000D-02 7.50000D-02 7.50000D-02 7.50000D-02 7.50000D-02 7.50000D-02  
1.00000D-01 1.00000D-01 1.00000D-01 1.00000D-01 1.00000D-01 1.00000D-01  
1.00000D-01 1.00000D-01 1.00000D-01 1.25000D-01 1.25000D-01 1.25000D-01  
1.25000D-01 1.25000D-01 1.25000D-01 1.25000D-01 1.25000D-01 1.25000D-01  
1.25000D-01 1.25000D-01 1.25000D-01 1.25000D-01 1.25000D-01 1.50000D-01  
1.50000D-01 1.50000D-01 1.50000D-01 1.50000D-01  
1.25000D-01 1.25000D-01 1.00000D-01 7.50000D-02 5.00000D-02 2.50000D-02  
2.50000D-02 5.00000D-02 5.00000D-02 7.50000D-02 7.50000D-02 7.50000D-02  
5.00000D-02 5.00000D-02 2.50000D-02 2.50000D-02

1.0 1.0 1.0  
1.0 1.0 1.0  
1.0 1.0 1.0  
1.0 1.0 1.0  
1.0 1.0 1.0  
1.0 1.0 1.0

-6.05115D-02 4.39628D-02-7.07061D-02 4.86296D-02-9.07488D-02 5.77973D-02  
-1.16465D-01 6.95511D-02-1.42718D-01 8.15449D-02-1.62778D-01 9.07081D-02  
-1.78412D-01 9.78492D-02-2.06010D-01 1.10457D-01-2.52712D-01 1.31796D-01  
-3.33809D-01 1.68875D-01-4.85594D-01 2.38349D-01-7.45917D-01 3.57679D-01  
-1.10192D 00 5.20969D-01-1.36075D 00 6.38583D-01-1.68462D-01 8.12709D-02  
9.23232D 00-4.29208D 00  
-5.24629D 01 2.43952D 01 3.30565D 00-1.52548D 00 9.59800D 00-4.44085D 00  
6.30965D 00-2.90579D 00 3.51748D 00-1.60596D 00 1.94227D 00-8.73900D-01  
9.67564D-01-4.22178D-01 4.56117D-01-1.86600D-01 2.33575D-01-8.53307D-02  
1.24716D-01-3.67737D-02 6.55499D-02-1.11698D-02 3.09838D-02 3.15938D-03  
7.02919D-03 1.24469D-02-8.37244D-03 1.76862D-02-1.63348D-02 1.96714D-02  
-2.00660D-02 1.98723D-02-2.13445D-02 1.90820D-02-2.11972D-02 1.77486D-02  
-2.02456D-02 1.61522D-02-1.89014D-02 1.44672D-02-1.74092D-02 1.28081D-02  
-1.57047D-02 1.10102D-02-1.39293D-02 9.15983D-03-1.23611D-02 7.50691D-03  
-1.10126D-02 6.04770D-03-9.86773D-03 4.76274D-03-8.89518D-03 3.63074D-03  
-8.06117D-03 2.64105D-03-7.33882D-03 1.77059D-03-6.69152D-03 1.00417D-03  
-6.10744D-03 3.31180D-04-5.56072D-03-2.68730D-04-5.03784D-03-7.98581D-04  
-4.53175D-03-1.27128D-03-4.03101D-03-1.70169D-03-3.46819D-03-2.14888D-03  
-2.82596D-03-2.64320D-03-2.13003D-03-3.23068D-03-1.27398D-03-4.26831D-03  
3.54277D-04-8.18834D-03

## TUBE END IMPEDANCE PROGRAM FOR UNFLANGED ANNULAR DUCT •

## INPUT DATA

A = 0.0                  B = 1.000000E 00    W = 3.430000E 02    S = 3.430000E 02

CHK= 9.999999E-05 RHO= 1.209999E 0C

L = 30    M = 16    N = 40    NN = 2    LP = 8    MW = 0    INK = 0

1.250000E-01	1.250000E-01	9.999996E-02	7.499999E-02
5.000000E-02	2.500000E-02	2.500000E-02	5.000000E-02
5.000000F-02	7.499999E-02	7.499999E-02	7.499999E-02
5.000000E-02	5.000000E-02	2.500000E-02	2.500000E-02

## OUTER DUCT WALL BOX LENGTHS

2.500000E-02	2.500000E-02	5.000000E-02	5.000000E-02
5.000000E-02	5.000000E-02	7.499999E-02	7.499999E-02
7.499999E-02	7.499999E-02	7.499999E-02	7.499999E-02
9.999996E-02	9.999996E-02	9.999996E-02	9.999996E-02
9.999996E-02	9.999996E-02	9.999996E-02	9.999996E-02
9.999996E-02	1.250000E-01	1.250000E-01	1.250000E-01
1.250000E-01	1.250000E-01	1.250000E-01	1.250000E-01
1.250000E-01	1.250000E-01	1.250000E-01	1.250000E-01
1.250000E-01	1.250000E-01	1.250000E-01	1.500000E-01
1.500000E-01	1.500000E-01	1.500000E-01	1.500000E-01

## THETA BOX WIDTH ON DUCT FACE

3.000000E-02	3.344828E-02	3.344828E-02	3.344828E-02
3.344828E-02	3.344828E-02	3.344828E-02	3.344828E-02
3.344828E-02	3.344828E-02	3.344828E-02	3.344828E-02
3.344828E-02	3.344828E-02	3.344828E-02	3.344828E-02
3.344828E-02	3.344828E-02	3.344828E-02	3.344828E-02
3.344828E-02	3.344828E-02	3.344828E-02	3.344828E-02
3.344828E-02	3.344828E-02	3.344828E-02	3.344828E-02
3.344828E-02	3.344828E-02	3.344828E-02	3.344828E-02

VELOCITY ON DUCT FACE

1.000000E 00	0.C	1.000000E 00	0.0
1.000000E 00	0.C	1.000000E 00	0.0
1.000000E 00	0.C	1.000000E 00	0.0
1.000000F 00	0.C	1.000000E 00	0.0
1.000000E 00	0.C	1.000000E 00	0.0
1.000000E 00	0.O	1.000000E 00	0.0
1.000000E 00	0.G	1.000000E 00	0.0
1.000000E 00	0.C	1.000000E 00	0.0

SOURCE DISTRIBUTION ON DUCT FACE.

-6.051150E-02	4.396280E-02	-7.070607E-02	4.862960E-02
-9.074879E-02	5.779730E-02	-1.164650E-01	6.955105E-02
-1.427180E-01	8.154488E-02	-1.627780E-01	9.070808E-02
-1.784120F-01	9.784919E-02	-2.060100E-01	1.104569E-01
-2.527120E-01	1.317959E-01	-3.338090E-01	1.688750E-01
-4.855940E-01	2.383490E-01	-7.459170E-01	3.576789E-01
-1.101919E 00	5.209690E-01	-1.360749E 00	6.385829E-01
-1.684620E-01	8.127087E-02	9.232320E 00	-4.292080E 00

SOURCE DISTRIBUTION ON OUTER DUCT WALL

-5.246289E 01	2.439519E 01	3.305650E 00	-1.525479E 00
9.558000E 00	-4.440849E 00	6.309649E 00	-2.905789E 00
3.517480E 00	-1.605960E 00	1.942269E 00	-8.739000E-01
9.675640E-01	-4.221780E-01	4.561170E-01	-1.866000E-01
2.335750F-01	-8.533067E-02	1.247160E-01	-3.677370E-02
6.554985E-02	-1.116980E-02	3.098380E-02	3.159380E-03
7.029187E-03	1.244690E-02	-8.372437E-03	1.768620E-02
-1.633480E-02	1.967140E-02	-2.006600E-02	1.987230E-02
-2.134450E-02	1.508200E-02	-2.119720E-02	1.774860E-02
-2.024560E-02	1.615220E-02	-1.890140E-02	1.446720E-02
-1.740920F-02	1.280810E-02	-1.570470E-02	1.101020E-02
-1.392930F-02	9.159829E-03	-1.236110E-02	7.506907E-03
-1.101260E-02	6.047700E-03	-9.867728E-03	4.762739E-03
-8.895177E-03	3.630740E-03	-8.061167E-03	2.641050E-03
-7.338818E-03	1.770590E-03	-6.691519E-03	1.004170E-03
-6.107438E-03	3.311799E-04	-5.560718E-03	-2.687299E-04
-5.037837E-03	-7.585809E-04	-4.531749E-03	-1.271280E-03
-4.031010F-03	-1.701690E-03	-3.468190E-03	-2.148880F-03
-2.825960E-03	-2.643200E-03	-2.130030E-03	-3.230680E-03
-1.273980F-03	-4.268307E-03	3.542770E-04	-8.188337E-03

INTEGRATION FOR BLOCK CENTERED AT THETA= 1.993285E-01 R= 6.250000E-02  
 DID NOT CONVERGE  
 REAL DIFF = 2.205372E-06 IMAG DIFF = 5.175781E-02

INTEGRATION FOR BLOCK CENTERED AT THETA= 6.083843E 00 R= 6.250000E-02  
 DID NOT CONVERGE  
 REAL DIFF = 2.324581E-06 IMAG DIFF = 5.171204E-02

ANNULAR RING NO 1 RADIAL POSITION = 6.250000E-02  
 LOCAL IMPEDANCE = 8.533759E 01 4.734263E 02  
 PRESSURE = 8.533759E 01 4.734263E 02  
 VELOCITY = 1.000000E 00 0.0

INTEGRATION FOR BLOCK CENTERED AT THETA= 6.083843E 00 R= 1.875000E-01  
 DID NOT CONVERGE  
 REAL DIFF = 3.814697E-06 IMAG DIFF = 1.831055E-04

ANNULAR RING NO 2 RADIAL POSITION = 1.875000E-01  
 LOCAL IMPEDANCE = 8.916052E 01 4.804661E 02  
 PRESSURE = 8.916052E 01 4.804661E 02  
 VELOCITY = 1.000000E 00 0.0

ANNULAR RING NO 3 RADIAL POSITION = 3.000000E-01  
 LOCAL IMPEDANCE = 9.621284E 01 4.936169E 02  
 PRESSURE = 9.621284E 01 4.936169E 02  
 VELOCITY = 1.000000E 00 0.0

ANNULAR RING NO 4 RADIAL POSITION = 3.874999E-01  
 LOCAL IMPEDANCE = 1.045224E 02 5.093547E 02  
 PRESSURE = 1.045224E 02 5.093547E 02  
 VELOCITY = 1.000000E 00 0.0

ANNULAR RING NO 5 RADIAL POSITION = 4.499999E-01  
 LOCAL IMPEDANCE = 1.123271E 02 5.243489E 02  
 PRESSURE = 1.123271E 02 5.243489E 02  
 VELOCITY = 1.000000E 00 0.0

INTEGRATION FOR BLOCK CENTERED AT THETA= 0.0 R= 5.124998E-01  
 DID NOT CONVERGE  
 REAL DIFF = 6.616116E-06 IMAG DIFF = 1.983643E-04

ANNULAR RING NO 6 RADIAL POSITION = 4.874998E-01  
 LOCAL IMPEDANCE = 1.179450E 02 5.352490E 02  
 PRESSURE = 1.179450E 02 5.352490E 02  
 VELOCITY = 1.000000E 00 0.0

INTEGRATION FOR BLOCK CENTERED AT THETA= 0.0 R= 4.874998E-01  
 DID NOT CONVERGE  
 REAL DIFF = 6.079674E-06 IMAG DIFF = 2.746582E-04

INTEGRATION FOR BLOCK CENTERED AT THETA= 0.0 R= 5.499998E-01  
 DID NOT CONVERGE  
 REAL DIFF = 5.722046E-06 IMAG DIFF = 3.356934E-04  
 ANNULAR RING NO 7 RADIAL POSITION = 5.124998E-01  
 LOCAL IMPEDANCE = 1.221649E 02 5.435139E 02  
 PRESSURE = 1.221649E 02 5.435139E 02  
 VELOCITY = 1.000000E 00 0.0

INTEGRATION FOR BLOCK CENTERED AT THETA= 0.0 R= 6.624997E-01  
 DID NOT CONVERGE  
 REAL DIFF = 1.621246E-05 IMAG DIFF = 1.678467E-04  
 ANNULAR RING NO 8 RADIAL POSITION = 5.499998E-01  
 LOCAL IMPEDANCE = 1.290967E 02 5.571472E 02  
 PRESSURE = 1.290967E 02 5.571472E 02  
 VELOCITY = 1.000000E 00 0.0

INTEGRATION FOR BLOCK CENTERED AT THETA= 0.0 R= 5.499998E-01  
 DID NOT CONVERGE  
 REAL DIFF = 1.144409E-05 IMAG DIFF = 1.220703E-04

INTEGRATION FOR BLOCK CENTERED AT THETA= 6.C83843E 00 R= 6.624997E-01  
 DID NOT CONVERGE  
 REAL DIFF = 1.811981E-05 IMAG DIFF = 2.136230E-04  
 ANNULAR RING NO 9 RADIAL POSITION = 5.999997E-01  
 LOCAL IMPEDANCE = 1.399527E 02 5.787158E 02  
 PRESSURE = 1.399527E 02 5.787158E 02  
 VELOCITY = 1.000000E 00 0.0

INTEGRATION FOR BLOCK CENTERED AT THETA= 6.C83843F 00 R= 6.624997E-01  
 DID NOT CONVERGE  
 REAL DIFF = 1.525879E-05 IMAG DIFF = 1.983643E-04  
 ANNULAR RING NO 10 RADIAL POSITION = 6.624997E-01  
 LOCAL IMPEDANCE = 1.565026E 02 6.119973E 02  
 PRESSURE = 1.565026E 02 6.119973E 02  
 VELOCITY = 1.000000E 00 0.0

INTEGRATION FOR BLOCK CENTERED AT THETA= 0.0 R= 6.624997E-01  
 DID NOT CONVERGE  
 REAL DIFF = 1.430511E-05 IMAG DIFF = 1.525879E-04

INTEGRATION FOR BLOCK CENTERED AT THETA= 0.0 R= 8.124996F-01  
 DID NOT CONVERGE  
 REAL DIFF = 2.574921E-05 IMAG DIFF = 4.272461E-04

INTEGRATION FOR BLOCK CENTERED AT THETA= 6.083843E 00 R= 7.374997E-01  
 DID NOT CONVERGE  
 REAL DIFF = 2.670288E-05 IMAG DIFF = 2.136230E-04

INTEGRATION FOR BLOCK CENTERED AT THETA= 6.083843E 00 R= 8.124996E-01  
 DID NOT CONVERGE  
 REAL DIFF = 2.384186E-05 IMAG DIFF = 2.288818E-04  
 ANNULAR RING NO 11 RADIAL POSITION = 7.374997E-01  
 LOCAL IMPEDANCE = 1.830660E 02 6.662146E 02  
 PRESSURE = 1.830660E 02 6.662146E 02  
 VELOCITY = 1.000000F 00 0.0

INTEGRATION FOR BLOCK CENTERED AT THETA= 0.0 R= 8.749996F-01  
 DID NOT CONVERGE  
 REAL DIFF = 6.675720E-06 IMAG DIFF = 2.136230E-04

INTEGRATION FOR BLOCK CENTERED AT THETA= 6.083843E 00 R= 7.374997E-01  
 DID NOT CONVERGE  
 REAL DIFF = 1.049042E-05 IMAG DIFF = 2.288818E-04  
 ANNULAR RING NO 12 RADIAL POSITION = 8.124996E-01  
 LOCAL IMPEDANCE = 2.218372E 02 7.467739E 02  
 PRESSURE = 2.218372E 02 7.467739E 02  
 VELOCITY = 1.000000E 00 0.0

INTEGRATION FOR BLOCK CENTERED AT THETA= 0.0 R= 8.124996E-01  
 DID NOT CONVERGE  
 REAL DIFF = 1.335144E-05 IMAG DIFF = 1.220703E-04

INTEGRATION FOR BLOCK CENTERED AT THETA= 1.993285E-01 R= 8.124996E-01  
 DID NOT CONVERGE  
 REAL DIFF = 1.621246E-05 IMAG DIFF = 1.983643F-04  
 ANNULAR RING NO 13 RADIAL POSITION = 8.749996E-01  
 LOCAL IMPEDANCE = 2.736311E 02 8.560786E 02  
 PRESSURE = 2.736311E 02 8.560786E 02  
 VELOCITY = 1.000000E 00 0.0

INTEGRATION FOR BLOCK CENTERED AT THETA= 0.0 R= 8.749996E-01  
 DID NOT CONVERGE  
 REAL DIFF = 1.335144E-05 IMAG DIFF = 1.831055E-04

INTEGRATION FOR BLOCK CENTERED AT THETA= 0.0 R= 9.624995E-01  
 DID NOT CONVERGE  
 REAL DIFF = 9.536743E-06 IMAG DIFF = 2.899170E-04  
 ANNULAR RING NO 14 RADIAL POSITION = 9.249995E-01  
 LOCAL IMPEDANCE = 3.457480E 02 1.010026E 03  
 PRESSURE = 3.457480E 02 1.010026E 03  
 VELOCITY = 1.000000E 00 0.0

INTEGRATION FOR BLOCK CENTERED AT THETA= 0.0 R= 9.249995E-01  
 DID NOT CONVERGE  
 REAL DIFF = 1.144409E-05 IMAG DIFF = 2.186584E-02

INTEGRATION FOR BLOCK CENTERED AT THETA= 0.0 R= 9.874995E-01  
 DID NOT CONVERGE  
 REAL DIFF = 7.629395E-06 IMAG DIFF = 2.427673E-02  
 ANNULAR RING NO 15 RADIAL POSITION = 9.624995E-01  
 LOCAL IMPEDANCE = 4.480442E 02 1.229231E 03  
 PRESSURE = 4.480442E 02 1.229231E 03  
 VELOCITY = 1.000000E 00 0.0

INTEGRATION FOR BLOCK CENTERED AT THETA= 0.0 R= 9.624995E-01  
 DID NOT CONVERGE  
 REAL DIFF = 6.675720E-06 IMAG DIFF = 2.485657E-02

INTEGRATION FOR BLOCK CENTERED AT THETA= 0.0 Z=-1.250000E-02  
 DID NOT CONVERGE  
 REAL DIFF = 4.768372E-06 IMAG DIFF = 7.092285E-02

INTEGRATION FOR BLOCK CENTERED AT THETA= 0.0 Z=-3.750000E-02  
 DID NOT CONVERGE  
 REAL DIFF = 5.722046E-06 IMAG DIFF = 1.831055E-04  
 ANNULAR RING NO 16 RADIAL POSITION = 9.874995E-01  
 LOCAL IMPEDANCE = 6.368638E 02 1.635084E 03  
 PRESSURE = 6.368638E 02 1.635084E 03  
 VELOCITY = 1.000000E 00 0.0

RESISTANCE RATIO, TAU = 0.51969945E 00  
 REACTANCE RATIO, CHI = 0.19329624E 01